THE JOURNAL OF BIOLOGICAL CHEMISTRY
© 2003 by The American Society for Biochemistry and Molecular Biology, Inc.

Vol. 278, No. 29, Issue of July 18, pp. 26704–26714, 2003
Printed in U.S.A.

Full Activation of Estrogen Receptor α Activation Function-1 Induces Proliferation of Breast Cancer Cells*

Received for publication, January 30, 2003, and in revised form, April 23, 2003
Published, JBC Papers in Press, May 8, 2003, DOI 10.1074/jbc.M301031200

Tetsuo Fujita‡§¶, Yoko Kobayashi‡¶, Osamu Wada‖, Yukiyo Tateishi‡, Lina Kitada‡, Yasuji Yamamoto, Hisashige Takashima‡, Akiko Murayama‡, Tetsu Yano‖, Tadashi Baba‡, Shigeaki Kato‡‡§§, Yoh-ichi Kawabe‡, and Junn Yanagisawa‡§¶¶**

*From the ‡Institute of Applied Biochemistry, University of Tsukuba, 1-1-1 Tenno-dai, Tsukuba Science City, Ibaraki 305-8572, the ‖Department of Obstetrics and Gynecology, Faculty of Medicine, University of Tokyo, 7-3-1 Hongo, Bunkyo-ku, Tokyo 113-8655, **Taiho Pharmaceutical Co., Ltd., Cancer Research Laboratory, Hanno Research Center, 1-27-1 Misugidai, Hanno City, Saitama 357-8527, ‡‡Institute of Molecular and Cellular Biosciences, University of Tokyo, 1-1-1 Yayoi, Bunkyo-ku, Tokyo 113-0034, §CREST, Japan Science and Technology, 4-1-8 Honcho, Kawaguchi, Saitama 332-0012, and §§SORST, Japan Science and Technology, 4-1-8 Honcho, Kawaguchi, Saitama 332-0012, Japan*

The effects of estrogen and anti-estrogen are mediated through the estrogen receptors (ER) α and β, which function as ligand-induced transcriptional factors. Recently, one of the phthalate esters, *n*-butylbenzyl phthalate (BBP), has been shown to induce estrogen receptor-mediated responses. By using the truncated types of ER mutants, we revealed that activation function-1 (AF-1) activity was necessary for the BBP-dependent transactivation function of ERα. AF-1 is also known to be responsible for the partial agonistic activity of tamoxifen. Whereas tamoxifen exhibits an anti-estrogenic effect on proliferation of the MCF-7 breast cancer cell line, BBP showed an estrogenic effect on MCF-7 to stimulate proliferation. *In vivo* and *in vitro* binding assays revealed that whereas 4-hydroxytamoxifen (OHT) induced binding of ERα to both an AF-1 coactivator complex (p68/p72 and p300) and corepressor complexes (N-CoR/SMRT), BBP selectively enhanced the binding to the AF-1 coactivators. We also showed that the transcriptional activity of OHT-bound ERα was modulated by the ratio between the AF-1 coactivator and corepressor complexes. Expression of a dominant-negative type of N-CoR inhibited the interaction between OHT-bound ERα and N-CoR/SMRT and enhanced the transcriptional activity of OHT-bound ERα. Furthermore, the cell growth of MCF-7 stably expressing the dominant-negative type of N-CoR was enhanced by the addition of OHT. These results indicated that fully activated AF-1 induces the stimulation of breast cancer growth and that the ratio between AF-1 coactivators and corepressors plays a key role to prevent proliferation of tumor by tamoxifen.

The effects of estrogens are mediated primarily via estrogen receptor α and β (ERα and -β),[1] which are members of the nuclear hormone receptor superfamily. Estrogen (E2) binding to its receptor induces the ligand binding domain to undergo a characteristic conformational change, whereupon the receptor dimerizes, binds to DNA, and subsequently stimulates gene expression (1–7). ERα is stimulated by two distinct activation regions, activation function-1 (AF-1) and AF-2 (2–4, 8). AF-1, which is located in the N-terminal A/B domain, is constitutively activated in a cell-specific and promoter-specific manner (9). AF-2 is located in the C-terminal ligand binding domain (LBD) and exerts ligand-dependent transcriptional activity (10). AF-1 and AF-2 activate transcription independently and synergistically and act in a promoter-specific and cell-specific manner (11).

The ligand-dependent activation of ERα requires ligand-dependent association of coactivator complexes (12–15). The coactivator complexes for AF-2 contain histone acetylases p300/CBP (16, 17), p300/CBP-associated factor (pCAF) (18), p160 protein family members steroid receptor coactivator-1 (SRC-1) (19, 20), transcription intermediary factor 2 (TIF2) (21), p300/CBP-interacting protein (p/CIP) (22–24), non-acetylase vitamin D receptor-interacting protein/TR-associated proteins (DRIP/TRAP) (25–29) or transformation/transcription domain-associated protein (TRRAP) (30–32), and general control of amino acid protein-5 (GCN5) (32, 33). AF-1 transcriptional activity is enhanced by p300 and DEAD box protein p68/p72, which form a protein complex with p160 family proteins and p300/CBP, and directly bind to the A/B domain to potentiate AF-1 activity (34, 35). The phosphorylation of the serine residue at position 118 in the A/B domain stabilizes the complex formation of ERα and the coactivator complex containing p68/p72 to potentiate the AF-1 activity (34–36).

Estrogen is known to stimulate hormone-dependent tumors such as endometrial cancer and breast cancer (37). Recently, it was suggested that some endocrine disrupters may also contribute to the development of hormone-dependent cancers (38, 39). Several studies have demonstrated that many endocrine disrupters, such as butylbenzyl phthalate (BBP), a phthalate ester used as a plasticizer, are capable of interacting with estrogen receptors and induce estrogen receptor-mediated responses, suggesting that estrogenic or anti-estrogenic effects elicited by these substances may be receptor-mediated (38–41).

* This work was supported by the 21st Century COE Program from the Ministry of Education, Culture, Sports, Sciences, and Technology (MEXT). The costs of publication of this article were defrayed in part by the payment of page charges. This article must therefore be hereby marked "*advertisement*" in accordance with 18 U.S.C. Section 1734 solely to indicate this fact.

¶ Both authors contributed equally to this work.

¶¶ To whom correspondence should be addressed. Tel.: 81-29-853-6632; Fax: 81-29-853-4675; E-mail: junny-tky@umin.ac.jp.

[1] The abbreviations used are: ER, estrogen receptor; AF, activation function; BBP, *n*-butylbenzyl phthalate; N-CoR, nuclear receptor corepressor; SMRT, silencing mediator for retinoid and thyroid hormone receptor; LBD, ligand binding domain; ID, interaction domain; OHT, 4-hydroxytamoxifen; ICI, ICI182,780; TSA, trichostatin A; GST, glutathione *S*-transferase; TK, thymidine kinase; ERE, estrogen-responsive element; DMEM, Dulbecco's modified Eagle's medium; FBS, fetal bovine serum; BrdUrd, 5-bromouridine 5′-triphosphate; E2, 17β-estradiol; SRC-1, steroid receptor coactivator-1; TRAP, TR-associated proteins; TRRAP, transformation/transcription domain-associated protein.

For the endocrine therapy of these cancers, the development of inhibitory ligands for ERs has yielded important therapeutic treatments, including the use of tamoxifen (37, 42, 43). Tamoxifen exhibits a wide range of estrogen-like and anti-estrogen actions according to the target tissue examined (44). While tamoxifen may exert anti-estrogenic activity by silencing the transcriptional activity of AF-2, agonist activity of tamoxifen can be mediated through AF-1 in a cell- or tissue-dependent manner (45–49). However, most patients undergoing long-term treatment of breast cancer with tamoxifen eventually experience recurrence of tumor growth. One of the reasons for this treatment failure is the acquisition by the tumor of the ability to respond to tamoxifen as a stimulatory rather than inhibitory ligand (50–53). Wolf *et al.* (54, 55) identified a mutant ERα from a tamoxifen-stimulated tumor that contained a point mutation that led to a tyrosine for aspartate substitution at amino acid 351 (ERα(D351Y)), located within the LBD of ERα (54, 55).

Recent studies (56–60) have suggested that tamoxifen promotes the binding of ERα to nuclear receptor corepressor (N-CoR) or related factors silencing mediator of retinoid and thyroid receptors (SMRT), which mediate repression by recruiting histone deacetylases (HDACs). We reported previously (61) that ERα(D351Y) exhibited reduced interaction with N-CoR and SMRT in the presence of 4-hydroxytamoxifen (OHT). These observations raised the possibility that OHT-dependent interaction between ERα and corepressor complexes may be essential for the anti-estrogenic effect of OHT and that abrogation of OHT-dependent binding of corepressors to ERα may convert OHT from antagonist to agonist to stimulate cancer growth.

In this paper, we identified BBP as an agonist for AF-1 of ERα. Although BBP exhibited the same properties as tamoxifen in a transient transfection assay, BBP-occupied ERα did not bind to corepressors and enhanced the proliferation of the breast cancer cell line MCF-7. The transcriptional activity of OHT-occupied ERα was modulated by the ratio of the expression levels between AF-1 coactivators and corepressors. Moreover, MCF-7 breast cancer cell lines expressing the dominant-negative type of N-CoR exhibited a growth phenotype in the presence of OHT. These results indicate that activation of AF-1 induces the stimulation of breast cancer growth and that the ratio between AF-1 coactivators and corepressors plays a key role to prevent proliferation of tumor by tamoxifen.

EXPERIMENTAL PROCEDURES

Materials—17β-Estradiol (E2) and OHT were purchased from Sigma. BBP was from Wako Chemicals Co., Japan. ICI182,780 (ICI) was synthesized by Taiho Pharmaceutical Co.

Measuring IC_{50} Values of E2 and BBP—For measurement of the binding constant value of BBP to ERα, IC_{50} measuring kit was purchased from Wako Chemicals Co., and IC_{50} was examined according to the manufacturer's protocol.

Plasmid Construction—The ERα/β expression plasmids (HEG0/ERG0β) and their deletion mutants (HE19/HE19β) were described previously (3, 11, 61, 64). The p300, p68, p72, SRC-1, TRAP220, and TRRAP expression plasmids were also described previously (32, 35, 62–64). Human N-CoR cDNA was cloned into pEF1-V5-His A for V5-N-CoR. Reporter constructs (17m5-luc, MH100-tk-luc, and ERE3-tk-luc) have been described previously (35, 61, 64). The ligand binding domain of ERα was inserted into the pM vector (Clontech) to generate GAL-DEF. VP-SRC-1, VP-TRAP220, and VP-p300 were described previously (11, 61, 64). Nuclear receptor interaction region in TRRAP was inserted into pVP16 vector to generate VP-TRRAP (32). C-terminal fragments of N-CoR and SMRT (including the NR interaction domains ID1 and ID2) were inserted into the pVP16 vector (Clontech) to generate VP-N-CoR, VP-SMRT, and pGEX-2T vector to GST-ID1-2 of N-CoR and SMRT and pcDNA3 vector (Invitrogen) for FLAG-N-CoR ID1-2. ERα mutation in amino acid replacement D351Y was introduced into full-length ERα and GAL-DEF plasmid by PCR-based point mutagenesis (Stratagene).

Transfection, Luciferase Assay, Mammalian Two-hybrid Assay, and Repression Assay—293T cells were maintained in Dulbecco's modified Eagle's medium (DMEM) supplemented with 10% fetal bovine serum (FBS). Two days before transfection, medium was changed to phenol red-free DMEM containing 5% charcoal-stripped FBS. Transfection was performed with Lipofectin reagent (Invitrogen) according to the manufacturer's protocol. For luciferase assays, 250 ng of ERE3-tk-luc plasmid was cotransfected with 25 ng of ER expression vector (HEG0/ERGβ0) or mutants. For mammalian two-hybrid assays, 250 ng of ERE3-tk-luc or 17m5-luc vector was cotransfected with 250 ng of HEG0, GAL-DEF, or GAL-DEF(D351Y) in combination with 250 ng of indicated VP16-conjugated constructs and/or p300, p68, N-CoR, or N-CoR ID1-2 plasmids. For repression analysis, 1 μg of MH100-tk-luc vector was cotransfected with 250 ng of GAL-DEF. As a reference plasmid to normalize for transfection efficiency, either 5 ng of pRL-CMV vector (Promega) or 125 ng of pRSVβGAL vector was cotransfected in all experiments. Six hours after transfection, culture medium was replaced with fresh medium containing 0.2% FBS. At this time, either E2 (10 nM), OHT (100 nM), ICI182,780 (100 nM), ethanolic vehicle, or 5 ng/ml trichostatin A (TSA) was added, and cells were incubated for an additional 24 h. Preparation of cell extracts and luciferase assays were performed following the manufacturer's protocol (Promega). β-Galactosidase activity was measured to control the efficiency for each transfection. Individual transfections, each consisting of triplicate wells, were repeated at least three times. For establishing MCF-7 stable transfectant of N-CoR ID1-2, Lipofectin reagent was used for introduce pcDNA-ID1-2, and transfectants were selected by 500 μg/ml G418 (Sigma), and several clones were isolated.

GST Pull-down Assay—For GST pull-down assays, bacterially expressed GST fusion proteins or GST bound to glutathione-Sepharose 4B beads (Amersham Biosciences) were incubated on ice with [^{35}S]methionine-labeled proteins expressed by *in vitro* translation using the TNT-coupled transcription-translation system (Promega). After 1 h of incubation, free proteins were removed by washing the beads 5 times with phosphate-buffered saline containing 10% glycerol and protease inhibitors (1 μg/ml aprotinin, 1 μg/ml leupeptin, and 1 μM phenylmethylsulfonyl fluoride). Specifically bound proteins were eluted by boiling in SDS sample buffer and analyzed by 6% SDS-PAGE. After electrophoresis, radiolabeled proteins were visualized by autoradiography.

Coimmunoprecipitation and Western Blotting—293T cells were transfected with the indicated plasmids, lysed in TNE (10 mM Tris-HCl (pH 7.8), 1% Nonidet P-40, 0.15 M NaCl, 1 mM EDTA, 1 μM phenylmethylsulfonyl fluoride, 1 μg/ml aprotinin) buffer, and immunoprecipitated with anti-FLAG M2 monoclonal antibody (Sigma) or anti-ERα (Chemicon). Interacting proteins were separated by 6% SDS-PAGE, transferred onto polyvinylidine difluoride membranes (Millipore), and detected with anti-ERα, anti-p300 (Santa Cruz Biotechnology), anti-FLAG M2, or anti-V5 tag (Invitrogen), and secondary antibodies were conjugated with horseradish peroxidase. For detecting the expression of ERα and N-CoR ID1-2, isolated clones were lysed in TNE, and each lysate was detected by immunoblotting using anti-ER or anti-FLAG and secondary antibodies.

Cell Proliferation Analysis—Two days before assay, MDA-MB-231 (ERα-negative) and MCF-7 (ERα-positive) cells were cultured in a 24-well plate in phenol red-free DMEM supplemented with 0.2% charcoal-stripped fetal bovine serum. As experimental medium, either E2 (10 nM), OHT (1 μM), BBP (1 μM), or ethanol vehicle was supplemented. Cells were harvested for the indicated times, and the number of viable cells was counted with hemocytometer.

S-phase Entry Analysis—For S-phase entry analysis, NIH3T3 cells were cultured in phenol red-free DMEM supplemented with 5% charcoal-stripped FBS and seeded onto glass coverslips at 60–70% confluence. Transfection with 3 μg of wild-type or mutant ERα expression plasmid was performed by using Perfectin Reagent (Gene Therapy Systems) according to the manufacturer's protocol. Incubation medium was changed after 24 h into phenol red-free DMEM supplemented with 0.2% charcoal-stripped FBS. Cells were left in this medium for 24 h and then cultured with 100 μM 5-bromouridine 5′-triphosphate (BrdUrd) in the presence of either E2 (10 nM), BBP (1 μM), or OHT (1 μM) for an additional 24 h. After incubation, the cells were fixed for immunostaining.

RESULTS

BBP Binds Ligand-binding Pocket of ERα and Induces the Transcriptional Activity of AF-1—It has been reported that BBP binds to ERα and enhances the transcriptional activity of ERα. To confirm the binding of BBP to ERs, we performed an *in vitro* competitive ligand binding assay to investigate the abilities of BBP to compete with E2 for binding to ERα and -β. E2

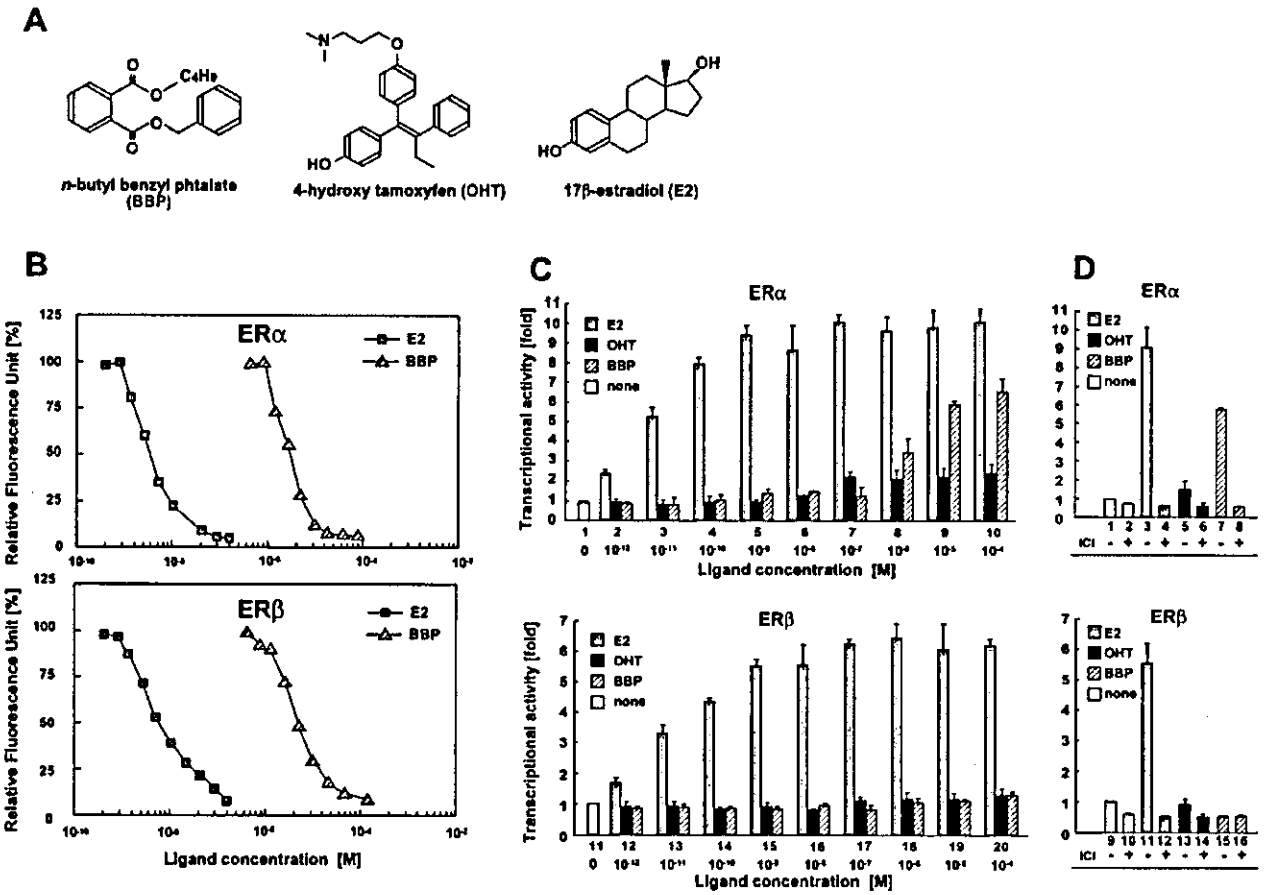

FIG. 1. **BBP enhances the transactivation function of ERα.** *A*, illustration of organic structures for BBP, OHT, and E2. *B*, BBP binds to the ligand pocket of ERs *in vitro*. Fluorescein-labeled estrogen bound to ERs was displaced competitively by increasing concentrations of E2 (*squares*) or BBP (*triangles*), and the ratio of displacement was measured using the luminescence meter. Displacement curves were obtained for E2 and BBP. The data were performed in triplicate and result from a representative experiment of the three repeated experiments. *C*, BBP enhances the transcriptional activity of ERα. 293T cells were transiently transfected with a plasmid expressing ERα (HEG0) or ERβ (ERG0β) and a reporter plasmid bearing 3× ER-responsive elements (ERE3-tk-luc) and incubated for 24 h with 10 fM to 100 μM of either E2, OHT, or BBP. Transcriptional activity of ERs was measured by luciferase assay. *Bars* indicate fold change in luciferase activity relative to that of no ligand. Results represent the average of three independent experiments; *error bars* indicate S.D. *D*, BBP-dependent transactivation of ERα is inhibited by ICI treatment. 293T cells were transfected with a plasmid expressing ERα (HEG0) or ERβ (ERG0β) and ERE3-tk-luc and incubated for 24 h in the presence of either E2 (10 nM), OHT (100 nM), or BBP (1 μM) with or without ICI (100 nM), and transcriptional activity was measured by luciferase assay. *Bars* indicate fold change in luciferase activity relative to that of no ligand. Results represent the average of three independent experiments; *error bars* indicate S.D.

exhibited an IC_{50} of ~1.0 nM to both ERs (Fig. 1*B*), which is within the range of previously reported IC_{50} values (40, 65). The IC_{50} values for BBP to ERα and ERβ were ~50 μM, indicating that BBP weakly bound to both receptors (Fig. 1*B*). Therefore, we next evaluated the ability of BBP to induce an ER-mediated response by measuring luciferase activity using 293T cells that were cotransfected with a luciferase reporter plasmid bearing estrogen response elements (EREs) and either ERα expression vector (HEG0) or ERβ expression vector (ERG0β). The results in Fig. 1, *C* and *D*, show that BBP treatment of 293T cells transiently transfected with ERα caused a concentration-dependent increase in luciferase activity. However, the transcriptional activity of ERβ was not enhanced by BBP treatment (Fig. 1*C*). E2 treatment of either ERα- or ERβ-transfected cells significantly induced luciferase activity (Fig. 1*C*). Induction of luciferase activity by BBP in transiently transfected 293T cells was completely abolished if the ERα construct, HEG0, was not cotransfected. In addition, 100 nM of the "pure ER antagonist" ICI182,780 completely inhibited BBP-induced transcriptional activity of ERα (Fig. 1*D*, *lanes 5* and *6*). These results indicate that BBP acts as an ERα-selective agonist. To investigate the reason why BBP stimulates the transcriptional activity of ERα but not ERβ, BBP-dependent transcriptional activity of truncated types of ERs (Fig. 2*A*) was estimated by luciferase assay. E2 enhanced the transcriptional activity of full-length ERα and a truncated type of ERα, HE19 (Fig. 2*B*, *lanes 2* and *6*), which does not have an A/B region and exhibits no AF-1 activity. In contrast, BBP stimulated only the transcriptional activity of full-length ERα (Fig. 2*B*), suggesting that AF-1 is essential for the BBP-dependent transcriptional activity of ERα. It is known that the non-steroidal anti-estrogen tamoxifen, which is the most commonly used endocrine in the treatment of all stages of breast cancer in both pre- and postmenopausal women, also exhibits AF-1 agonistic activity (45–49). In this experiment, OHT induced full-length ERα-mediated transcriptional activity (Figs. 1*C* and 2*B*) but did not stimulate the transcriptional activity of HE19 (Fig. 2*B*), as expected. The transcriptional activity induced by BBP was about three times higher than that induced by OHT (Fig. 2*B*, compare *lane 3* to *4*). These results raise the possibility that BBP may possess the same biological properties as tamoxifen.

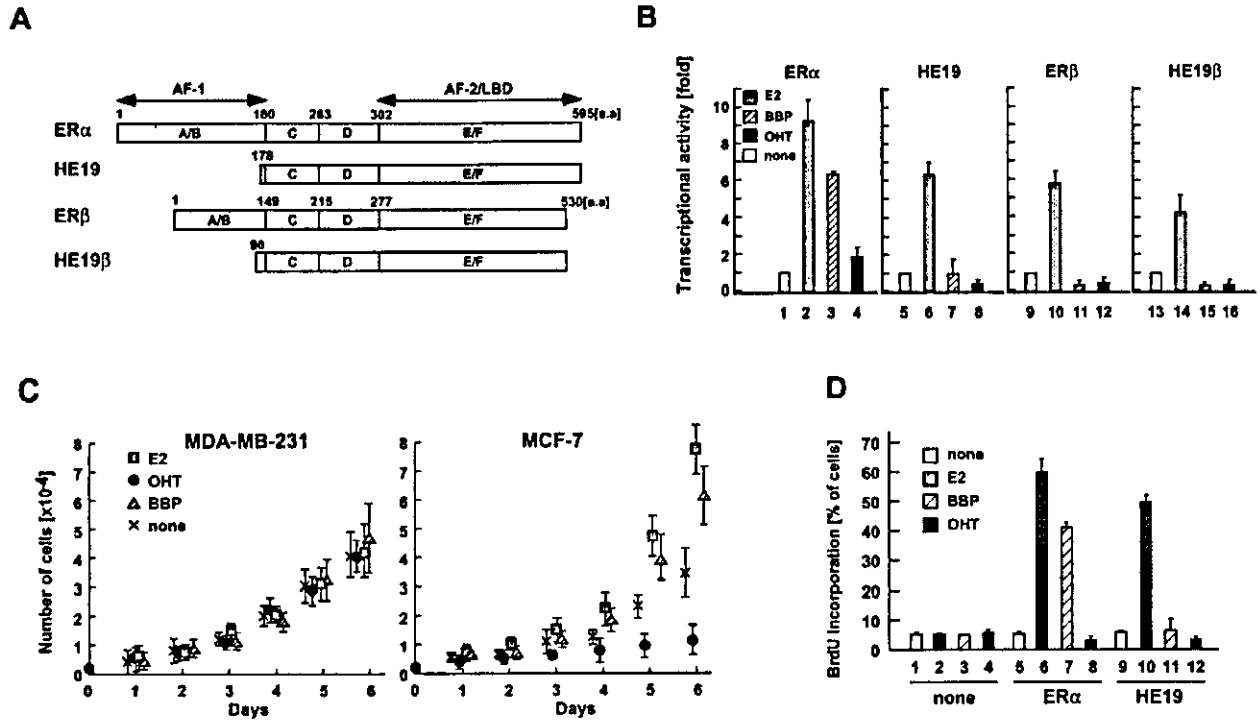

FIG. 2. **A contrastive effect between BBP and OHT on proliferation of breast cancer cells.** *A*, schematic representations of ERα expressed from HEG0 and HE19 and ERβ from ERG0β and HE19β. HE19 encodes truncated ERα defecting the N-terminal 1–177 amino acids and HE19β encodes truncated ERβ defecting 1–89 amino acids concerned with AF-1 activity. *B*, BBP- and OHT-dependent transactivation of ERα requires the ERα AF-1 activity. Expression plasmids of ERs (HEG0/ERG0β) or truncated ERs (HE19/HE19β) were transfected into 293T cells with ERE3-tk-luc in the absence (none) or presence of either E2 (10 nM), OHT (100 nM), or BBP (1 μM). *C*, BBP but not OHT stimulates proliferation of the breast cancer cell line MCF-7. MCF-7 and MDA-MB-231 cells were cultured for the indicated times in the absence (none) (*crosses*) or presence of either E2 (10 nM) (*squares*), OHT (1 μM) (*circles*), or BBP (1 μM) (*triangles*), and the number of viable cells was counted. Data are shown as means ± S.D. of triplicate cultures. *D*, BBP-dependent S-phase entry requires ERα AF-1 activity. NIH3T3 fibroblasts transfected with either HEG0 or HE19 were made quiescent and then left unstimulated (none) or stimulated with either E2 (10 nM), OHT (1 μM), or BBP (1 μM). BrdUrd was incubated in the cell medium, and its incorporation into DNA was assessed by immunofluorescent staining. Several coverslips were analyzed, and data from at least 200 scored cells were represented according to the formula: percentage of BrdUrd-positive cells = (number of BrdUrd-positive cells/number of transfected cells) × 100. In each case, the BrdUrd incorporation of non-transfected fibroblasts was evaluated and subtracted.

A Contrastive Effect between BBP and OHT on the Proliferation of Breast Cancer Cells—Thus, we next examined the effects of BBP on proliferation of two human breast cancer cell lines: MCF-7 and MDA-MB-231. The MCF-7 cell line expresses ERs, and its proliferation is estrogen-dependent. MDA-MB-231 cells, whose growth is not affected by estrogens, were used to control for false-positive responses. Whereas E2 induced MCF-7 cell proliferation at concentrations at 10 nM, OHT strongly inhibited the proliferation of MCF-7 cells (Fig. 2*C*, *right panel*) (41). In contrast with OHT, BBP exerted an increase in MCF-7 proliferation at 1 to 10 μM, and the maximum effect represented 70% of the presence of E2 (Fig. 2*C*, *right panel*). None of the three compounds we tested affected proliferation of MDA-MB-231, which does not express ERα (Fig. 2*C*, *left panel*).

To investigate whether the AF-1 activity is necessary for the BBP-dependent cell proliferation, newly synthesized DNA was evaluated by BrdUrd incorporation method. NIH3T3 fibroblasts were transiently transfected with expression plasmid encoding either ERα (HEG0) or ERα mutant (HE19). The transfected NIH3T3 fibroblasts were made quiescent and then stimulated for 24 h with either E2, BBP, or OHT (86). BrdUrd was added to the medium together with the ligands, and its incorporation into DNA was analyzed. BrdUrd-positive cells expressing either ERα or HE19 were counted. The NIH3T3 cells transfected with control vector did not respond to ligand treatments. Although E2 and BBP strongly stimulated progression of ERα-transfected NIH3T3 cells toward S-phase, BrdUrd incorporation into HE19-transfected cells was enhanced by E2 but not by BBP (Fig. 2*D*). These results indicate that the BBP-dependent S-phase entry requires the AF-1 activity of ERα.

BBP and OHT Induce the Binding of ERα to AF-1 Coactivators but Not to AF-2 Coactivators—Our results indicate that both BBP and OHT are selective agonists for ERα AF-1 and show an antagonistic effect on AF-2, whereas BBP exhibits an estrogenic effect and OHT shows an anti-estrogenic effect on the cell proliferation. In order to reveal a reason for this discrepancy, we tested the interaction between ERα and coactivators or corepressors in the presence of either BBP or tamoxifen. By using a mammalian two-hybrid assay, we first evaluated the BBP- or OHT-dependent binding of AF-1 coactivators to ERα. HEG0 was cotransfected with either VP16 transactivation domain-fused p72 (VP-p72), p68 (VP16-p68), or p300 (VP-p300) constructs into 293T cells. All of the three ligands we tested induced the interaction of ERα with either p68, p72, or p300 (Fig. 3*A*). The BBP-dependent interaction between ERα and AF-1 coactivators was confirmed using a coimmunoprecipitation method. By using an anti-ERα antibody, ERα was immunoprecipitated from a nuclear extract of 293T cells that were cotransfected with ERα and either FLAG-tagged p72, FLAG-tagged p68, or p300. Strong anti-FLAG or anti-p300 antibody binding was observed on immunoblots of anti-ERα immunoprecipitates from cotransfectants treated with either E2, BBP, or OHT (Fig. 3*B*).

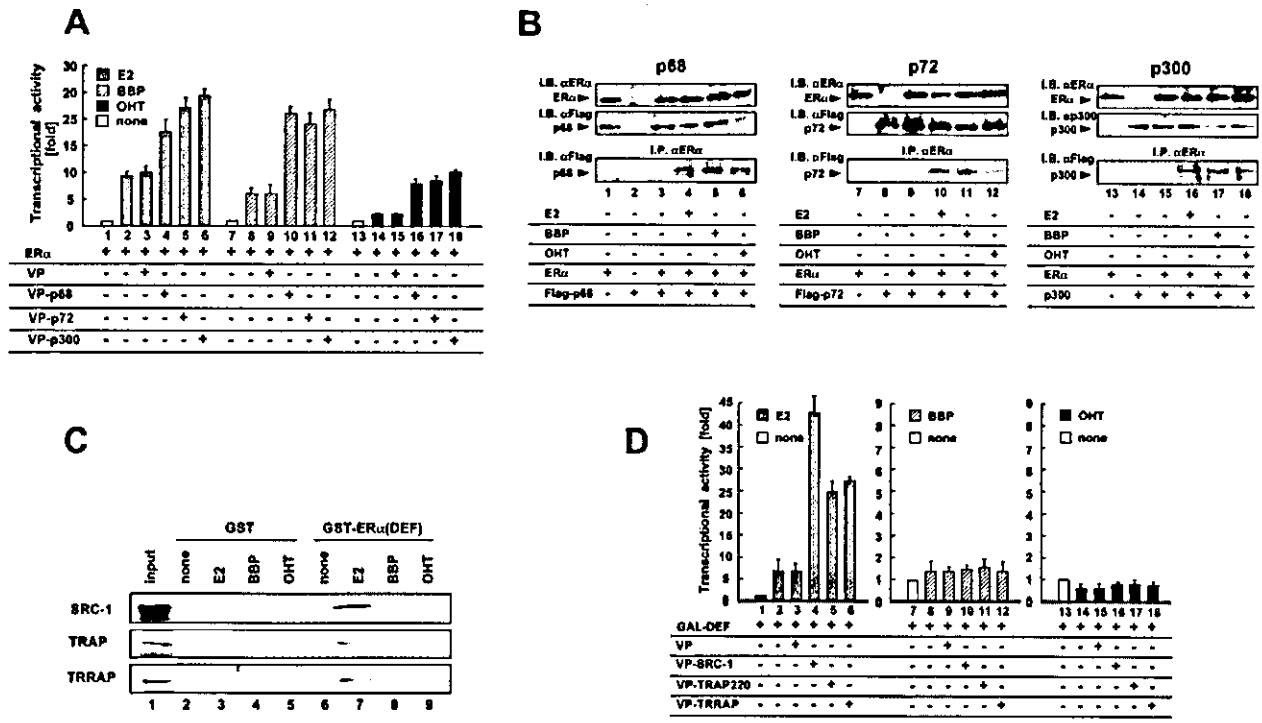

FIG. 3. **OHT and BBP induce the binding of AF-1-specific coactivators to ERα.** *A*, recruitment of AF-1 coactivators to BBP- or OHT-occupied ERα. Mammalian two-hybrid assays using ERα, along with either VP-p68, VP-p72, VP-p300, or VP, were performed. Indicated plasmids were transfected into 293T cells with HEG0 and ERE3-tk-luc in the absence (none) or presence of either E2 (10 nM), OHT (100 nM), or BBP (1 μM). *Bars* show fold change in luciferase activity relative to HEG0 and VP vectors in the absence of ligands. Results represent the average of three independent experiments; *error bars* indicate S.D. *B*, confirmation of OHT- and BBP-induced binding between ERα and p68/p72/p300 by coimmunoprecipitation. Nuclear extracts were prepared from 293T cells coexpressing ERα and FLAG-tagged p68, FLAG-tagged p72, or p300. ERα was then immunoprecipitated by anti-ERα antibody, and immunoprecipitates were detected by immunoblotting with anti-FLAG or anti-p300 antibody. *C*, BBP or OHT does not induce the binding of ERα to AF-2 coactivators *in vitro*. GST pull-down assays were performed using GST or GST-fused ERα DEF region produced by *Escherichia coli* with either [^{35}S]methionine-labeled SRC-1, TRAP220, or TRRAP translated *in vitro* in the presence of either E2 (10 nM), OHT (100 nM), or BBP (1 μM). *D*, BBP or OHT does not induce the binding of ERα to AF-2 coactivators *in vivo*. Mammalian two-hybrid assays using ERα (GAL-DEF), along with either SRC-1 (VP-SRC-1), TRAP220 (VP-TRAP220), or TRRAP (VP-TRRAP) were performed. Indicated plasmids were transfected into 293T cells with ERE3-tk-luc in the absence (none) or presence of either E2 (10 nM), OHT (100 nM), or BBP (1 μM). *Bars* show fold change in luciferase activity relative to GAL-DEF and VP vectors in the absence of ligands. Results represent the average of three independent experiments; *error bars* indicate S.D.

We then examined the binding of the DEF region of ERα with AF-2 coactivators. A GST pull-down assay showed that whereas E2 induced the direct binding of ERα(GAL-DEF) to AF-2 coactivators SRC-1, TRAP220, or TRRAP, BBP and OHT abrogated the interaction between GAL-DEF and AF-2 coactivators (Fig. 3*C*). In a mammalian two-hybrid experiment, E2-bound GAL-DEF exhibited significant binding to either SRC-1, TRAP220, or TRRAP (Fig. 3*D*, *left panel*). Conversely, neither BBP nor OHT induced the interaction between GAL-DEF and AF-2 coactivators (Fig. 3*D*, *middle* and *right panels*). These results were in good agreement with the observation that BBP and OHT act as antagonists for AF-2.

OHT but Not BBP Induces the Interaction between ERα and Corepressor Complexes—In a previous paper, we showed that OHT induces the binding between GAL-DEF and corepressor complexes to repress the basal transcriptional activity of TK promoter located downstream from GAL4-binding elements (17 × 5 m) (61). This OHT-induced binding of ERα to corepressor complexes is reduced by the amino acid substitution at position 351 in ERα (ERα(D351Y)), which is derived from tamoxifen-induced tumor (Fig. 4*A*) (54, 55). Consistent with previous studies, OHT-bound GAL-DEF repressed the transcriptional activity of the TK promoter (Fig. 4*B*, *lane 2*). This repressive activity was inhibited by the addition of TSA, a specific histone deacetylase inhibitor (Fig. 4*B*, *lane 5*). The D351Y mutation, which exhibited decreased corepressor association, impaired the tamoxifen-dependent repression by GAL-DEF (Fig. 4*B*, *lane 8*). In the presence of BBP, the repressive activity of GAL-DEF was not observed (Fig. 4*B*, *lane 3*), indicating that BBP-bound ERα would not interact with corepressor complexes.

To test the interaction between ERα and corepressors, a mammalian two-hybrid assay was performed. Either GAL-DEF or GAL-DEF(D351Y) was cotransfected into 293T cells with either VP, VP-SMRT, or VP-N-CoR. Whereas the interaction between GAL-DEF and corepressors was observed in the presence of OHT (Fig. 4*C*, *middle panel*), BBP-bound GAL-DEF exhibited no binding to corepressors as expected (Fig. 4*C*, *right panel*). Consistent with previous studies, the D351Y mutation reduced the OHT-induced interaction with corepressors (Fig. 4*C*, *lanes 10–12*) (61). The corepressor binding was further investigated by a coimmunoprecipitation method. By using an anti-ERα antibody, ERα was immunoprecipitated from nuclear extracts of 293T cells that were cotransfected with ERα and V5-tagged N-CoR. In the presence of OHT, anti-V5 antibody binding was observed on immunoblots of anti-ERα immunoprecipitates from cotransfectants (Fig. 4*D*, *lane 5*). In contrast, N-CoR was not coprecipitated with E2- or BBP-bound ERα (Fig. 4*D*, *lanes 4* and *6*).

The Ratio of AF-1 Coactivator/Corepressor Complexes in Cells Is an Essential Determinant for the Transcriptional Activity of OHT-occupied ERα—Our results indicated that al-

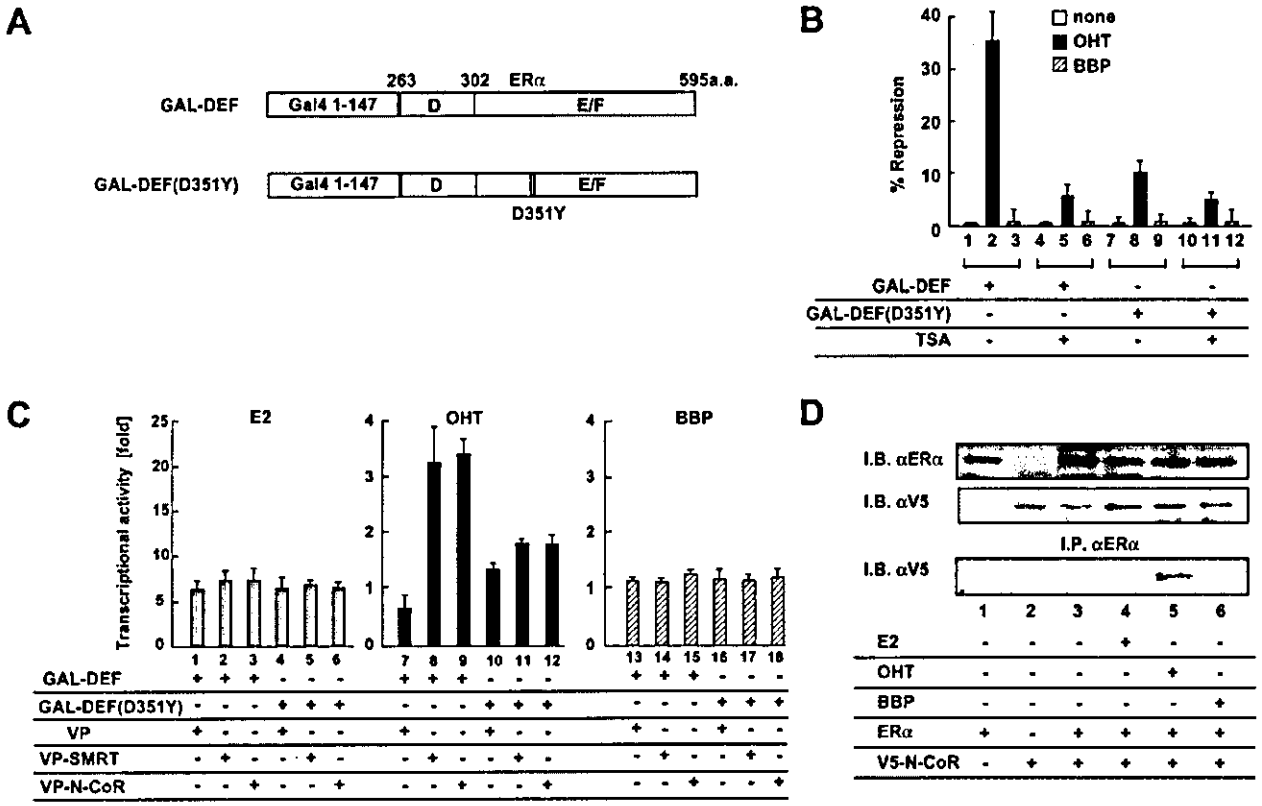

FIG. 4. **OHT but not BBP induces the binding of corepressor complexes to ERα.** *A*, schematic representation of GAL-DEF and GAL-DEF(D351Y). Ligand binding domain of wild-type ERα (263–595 amino acids (*a.a.*)) and ERα amino acid substitution D351Y were fused with GAL4 DNA binding domain. *B*, repressive activity of ERα AF-2 is induced by OHT but not by BBP. Indicated plasmids were transfected into 293T cells along with a reporter plasmid bearing GAL4-binding elements and the TK promoter (MH100-tk-luc) in the absence (none) or presence of OHT (100 nM), BBP (1 μM), or TSA (5 ng/ml). *Bars* indicate the repression rate of luciferase activity relative to GAL-DEF in the absence of ligands. Results represent the average of three independent experiments; *error bars* indicate S.D. *C*, BBP does not induce the binding of ERα to corepressors *in vivo*. Mammalian two-hybrid assays were performed using either GAL-DEF or GAL-DEF(D351Y), along with either VP-N-CoR, VP-SMRT, or VP. Indicated plasmids were transfected into 293T cells with a reporter plasmid bearing GAL4-binding elements (17m5-luc) in the absence (none) or presence of either E2 (10 nM), OHT (100 nM), or BBP (1 μM). *Bars* indicate fold change in luciferase activity relative to the GAL-DEF and VP vectors. Results represent the average of three independent experiments; *error bars* indicate S.D. *D*, the confirmation of OHT- and BBP-induced binding between ERα and N-CoR by coimmunoprecipitation. Nuclear extracts were prepared from 293T cells coexpressing ERα and V5-tagged N-CoR. ERα was immunoprecipitated by anti-ERα antibody, and V5-N-CoR in the anti-ERα immunoprecipitates was detected by immunoblotting with anti-V5 antibody.

though OHT induced the binding of ERα to both AF-1 coactivators and corepressors, BBP-bound ERα selectively associated with AF-1 coactivators. Thus we next examined the effect of AF-1 coactivators and corepressors on transcriptional activity of ERα induced by OHT or BBP. The expression of p300 and p68 enhanced the transcriptional activity of ERα in the presence of E2, OHT, or BBP (Fig. 5*A*). On the contrary, N-CoR reduced OHT-dependent transactivation function of ERα (Fig. 5*B*, *middle panel*) but not E2- and BBP-dependent activation (Fig. 5*B*, *left* and *right panels*). The stimulation of OHT-dependent transcriptional activity of ERα(D351Y) by the expression of AF-1 coactivators was much higher than that of wild-type ERα (Fig. 5*A*, compare *left* to *middle panel*), suggesting that the association of endogenous corepressor complexes with OHT-bound ERα reduces AF-1 activity. The maximum OHT-dependent transcriptional activity induced by coactivator expression was comparable with the BBP-dependent activity (Fig. 5*A*, compare *lanes 14–16*), raising the possibility that the overexpression of coactivators may convert OHT from antagonist into agonist to stimulate cancer growth. In addition, as shown in Fig. 5*D*, enhancement of transcriptional activity by the coactivator expression was reduced by the expression of corepressor, N-CoR. These findings indicate that the ratio of coactivator/corepressor in cells determines the transcriptional activity of OHT-bound ERα and that the inhibition of corepressor binding to ERα may convert OHT from partial agonist to full agonist for AF-1 to stimulate cell growth of MCF-7.

Inhibition of the Interaction between OHT-bound ERα and Corepressors Stimulates Proliferation of Breast Cancer Cells in the Presence of OHT—To investigate this hypothesis, we first determined the regions in N-CoR/SMRT, which are responsible for the interaction between N-CoR/SMRT and OHT-occupied ERα. Recently, it was shown that retinoid X receptor and TR LBDs associate with N-CoR/SMRT via the N-CoR/SMRT domains ID1 and ID2 (66–69). Therefore, we assessed whether GST-ID1-2 fusion proteins could associate with *in vitro* translated ERα. A GST pull-down assay showed both GST-ID1-2 derived from N-CoR and SMRT directly bound to ERα in the presence of OHT (Fig. 6*B*). We then studied whether the expression of the ID1-2 region abrogates the interaction between OHT-occupied ERα and N-CoR/SMRT using a mammalian two-hybrid assay. In this assay, the binding of N-CoR/SMRT to OHT-bound ERα was inhibited by the expression of the ID1-2 region derived from N-CoR (Fig. 6*C*). Coexpression of the ID1-2 region with ERα enhanced the OHT-dependent transactivation function of ERα (Fig. 6*D*, *left panel*) but not that of ERα(D351Y)

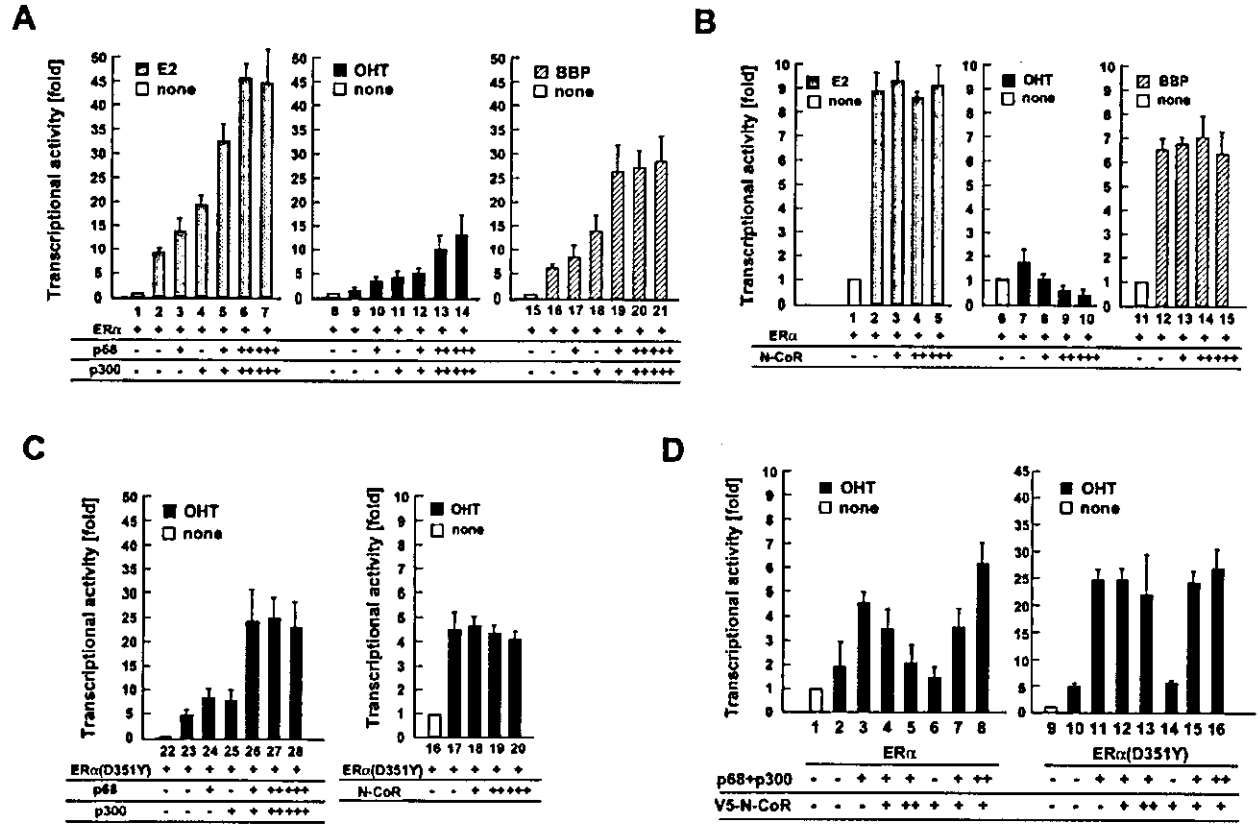

FIG. 5. **A competitive effect between AF-1 coactivator and corepressor complexes on the OHT-induced transcriptional activity of ERα.** *A*, E2-, OHT-, or BBP-dependent transcriptional activity is enhanced by expression of AF-1 coactivators. Indicated plasmids were transfected into 293T cells with HEG0 and ERE3-tk-luc in the presence of E2 (10 nM), OHT (100 nM), or BBP (1 μM). The amount of transfected plasmids for p68/p300 was 0.25 (+), 0.5 (++), and 1.0 μg (+++), respectively. *Bars* indicate fold change in luciferase activity relative to ERα in the absence of ligand. Results represent the average of at least three independent experiments; *error bars* indicate S.D. *B*, OHT-induced transcriptional activity is reduced by expression of N-CoR. Indicated plasmids were transfected into 293T cells with HEG0 and ERE3-tk-luc in the presence of either E2 (10 nM), OHT (100 nM), or BBP (1 μM). The amount of transfected plasmids for N-CoR was 0.25 (+), 0.5 (++), and 1.0 μg (+++), respectively. *Bars* indicate fold change in luciferase activity relative to ERα in the absence of ligand. *C*, effects of AF-1 coactivators and corepressors on OHT-induced transcriptional activity of ERα(D351Y). Indicated plasmids were transfected into 293T cells with ERE3-tk-luc in the presence of OHT (10 nM). The amount of transfected plasmids for p68/p300 and N-CoR was 0.25 (+), 0.5 (++), and 1.0 μg (+++), respectively. *Bars* indicate fold change in luciferase activity relative to ERα in the absence of ligands. *D*, the ratio between AF-1 coactivators and corepressors regulates the OHT-dependent transcriptional activity. Indicated plasmids were transfected into 293T cells with ERE3-tk-luc in the presence of OHT (100 nM). The amount of transfected plasmids for p68/p300 and N-CoR was 0.25 (+) and 0.5 μg (++), respectively. *Bars* indicate fold change in luciferase activity relative to ERα in the absence of ligand.

(Fig. 6*D*, *right panel*), indicating that the inhibition of corepressor binding enhances the AF-1 activity of ERα.

Next, we examined the effect of the expression of the ID1-2 region on the E2-dependent growth phenotype of the MCF-7 breast cancer cell line. The expression vector containing FLAG-tagged ID1-2 region was transfected into MCF-7 cells, and several stable cell lines constitutively expressing the ID1-2 region in MCF-7 cells (MCF-7(ID1-2)) were established. We picked up four independent clones, clones 1–4, and we examined the expression of ERα and ID1-2 by Western blot using specific antibodies against ERα and FLAG epitope. In all four clones we tested, the expression of FLAG-ID1-2 was observed (Fig. 7*A*). The expression level of ERα in these clones was unchanged when compared with the control MCF-7 cells (Fig. 7*A*). In the absence of E2, ID1-2 stable clones exhibited normal cell growth similar to the control MCF-7 (Fig. 7*B*). However, either E2 or BBP treatment enhanced the growth rate of the control and clones. OHT inhibited the growth of control MCF-7 cells but stimulated the growth of ID1-2 stable transformants (Fig. 7*B*), indicating that the inhibition of corepressors binding to ERα converts OHT from anti-estrogenic to an estrogenic effect on the proliferation of breast cancer cells.

DISCUSSION

BBP is a phthalic ester that is present in papers and paperboards used as packaging materials for aqueous, fatty, and dry foods (38, 40, 41). BBP has been shown to possess estrogenic properties *in vitro* and *in vivo* (40, 41). We showed that whereas BBP bound to ERα and ERβ, it stimulated the transcriptional activity of ERα but not that of ERβ. The results obtained from the experiments using the truncated type of ERα, HE19, revealed that the A/B region of ERα was responsible for the transactivation induced by BBP. This property of BBP resembles the property of tamoxifen which engenders a conformational change in the ligand binding domain distinct from that induced by E2 and inhibits the activity of the hormone-dependent AF-2 but not AF-1 (70, 71). Whereas both BBP and tamoxifen acted as an AF-1-selective agonist, BBP and tamoxifen exhibited a contrastive effect on proliferation of the breast cancer cell line MCF-7. OHT showed an anti-estrogenic effect on MCF-7 cells, and BBP had an estrogenic effect to stimulate proliferation of MCF-7.

The Structure of LBD Induced by BBP Is Different from That Induced by OHT—Accumulating evidence suggests that the

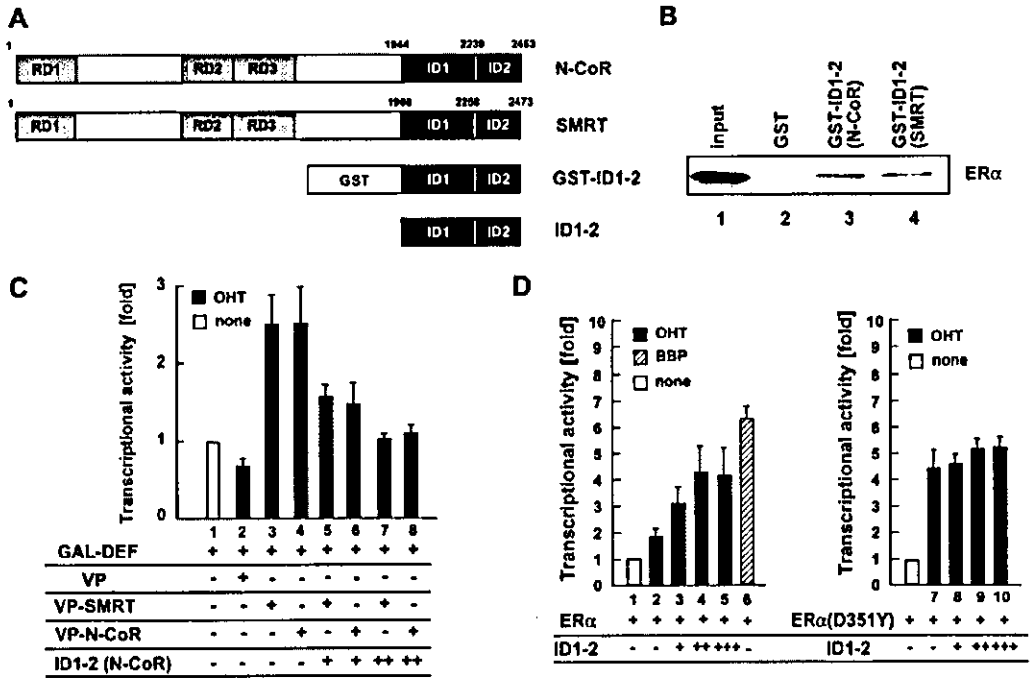

FIG. 6. **Overexpression of the N-CoR ID1-2 region abrogates the binding of corepressor complexes to OHT-occupied ERα.** *A*, schematic representation of corepressors N-CoR/SMRT. *B*, OHT induces the binding of the ID1-2 region of N-CoR/SMRT to ERα *in vitro*. GST pull-down assays were performed using GST or GST-fused ID1-2 region of N-CoR or SMRT produced by *E. coli* and [^{35}S]methionine-labeled ERα translated *in vitro* in the presence of OHT (100 nM). *C*, expression of ID1-2 region abrogates the binding between OHT-occupied ERα and corepressors. Mammalian two-hybrid assays were performed using GAL-DEF along with either VP-N-CoR, VP-SMRT, or VP. Indicated plasmids were transfected into 293T cells with 17m5-luc in the presence of OHT (100 nM). OHT-induced interactions between ERα and N-CoR/SMRT were inhibited by cotransfection of 0.25 (+) or 0.5 μg (++) of an ID1-2 expressing plasmid. *Bars* indicate fold change in luciferase activity relative to the GAL-DEF and VP vectors in the absence of ligand. Results represent the average of at least three independent experiments; *error bars* indicate S.D. *D*, expression of ID1-2 region stimulates OHT-dependent transcriptional activity. Indicated plasmids were transfected into 293T cells with ERE3-tk-luc in the presence of OHT (100 nM). OHT-induced transcriptional activity was enhanced by cotransfection of 0.25 (+), 0.5 (++), or 1.0 μg of an ID1-2 expressing plasmid. *Bars* indicate fold change in luciferase activity relative to ERα plasmids in the absence of ligand. Results represent the average of at least three independent experiments; *error bars* indicate S.D.

differential ability of partial antagonists to modify gene expression cannot be accounted for by alterations in the ligand-receptor complex alone but also must take into consideration coregulator (coactivator and corepressor) proteins that regulate ER interaction with the general transcriptional machinery and chromatin (15, 32, 59, 72–75). Therefore, coactivators and corepressors of the ERα were tested to determine whether these coregulators interact with ERα in the presence of these compounds. All of the three compounds we tested induced the interaction between ERα and AF-1 coactivators p68/p72 and p300 as expected. E2 induced the binding of LBD to AF-2 coactivators but not to corepressors (32, 59, 74, 75, 78). Consistent with previous reports (70, 71), OHT induced the interaction with corepressors instead of AF-2 coactivators. In contrast, BBP-occupied LBD bound to neither AF-2 coactivators nor corepressors.

The crystal structures of the LBDs of several nuclear receptors have been determined and described as a sandwich of 12 α-helices (H1–H12) with a central hydrophobic ligand-binding pocket (70, 71, 76, 77). In the presence of ligands, the hinge region between H11 and H12 is moved closer to H3 and H5, and H12 is positioned over the ligand-binding pocket formed by H3, H4, and H5. The repositioned H12 releases the corepressors from the LBD and forms a hydrophobic groove with H3 and H5 (70, 71). This hydrophobic groove is known to be important for interaction with LXXLL motifs found in p160 family members (SRC-1, transcription intermediary factor 2, and p300/CBP-interacting protein) as well as in other coactivator molecules (49, 71, 79, 80). The structures of tamoxifen-bound ERα revealed that the position of H12 differed compared with that of H12 in E2-bound ERα and did not form a coactivator interaction surface but a recognition surface for corepressor complexes (70, 71). We observed that BBP induced the binding of LBD to neither AF-2 coactivators nor corepressors, indicating that the position of H12 in BBP-bound ERα is different from that of H12 in E2- or OHT- bound ERα. These results also suggest that the structural differences induced by compound binding would affect the binding affinity of ERα to the coregulators.

The Ratio between AF-1 Coactivator and Corepressor Complexes in Cells Is a Major Determinant of the Transactivation of OHT-occupied ERα—Our results indicated that OHT induced the binding of ERα to both AF-1 coactivators and corepressors. The enhancement of transcriptional activity induced by coactivator expression was reduced by the corepressor expression, indicating that the ratio of coactivator/corepressor in cells determines the transcriptional activity of OHT-bound ERα. It is well known that p300 possesses histone acetyltransferase activity that modifies local chromatin structure into a transcriptionally permissive state (16, 17). N-CoR/SMRT complexes contain histone deacetylase activity (62, 81–83), suggesting that AF-1 coactivator and corepressor complexes may act and/or bind competitively to tamoxifen-bound ERα. If the OHT-occupied ERα simultaneously binds coactivators and corepressors under these conditions, the repressor domain of corepressors may inhibit ERα transcriptional activity by blocking the activation function of coactivators. Alternatively, OHT may induce competitive binding between AF-1 coactivators and corepressors to abrogate full AF-1 activity. OHT may induce an LBD

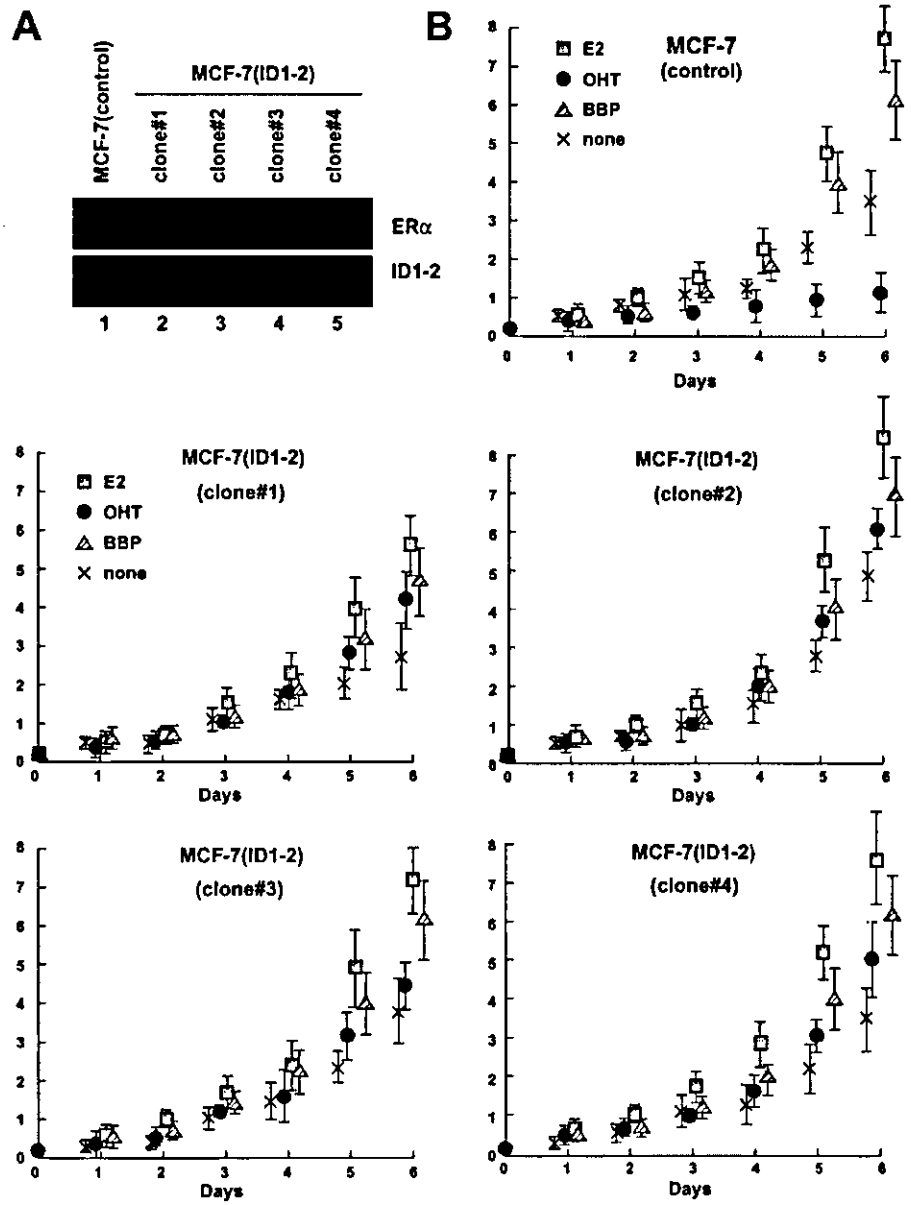

FIG. 7. **The breast cancer cell lines expressing the ID1-2 region exhibit OHT-stimulated growth phenotype.** *A*, expression levels of the ID1-2 region of N-CoR in ID1-2 stable transfectants (*clone 1–4*) measured by immunoblotting. Equal protein loading were ensured by ERα levels. *B*, MCF-7 stably expressing ID1-2 region exhibits the OHT-stimulated growth phenotype. Control MCF-7 cells and MCF-7 cell lines stably expressing the ID1-2 region (*clones 1–4*) were cultured for the indicated times in the absence (none) (*crosses*) or presence of either E2 (10 nM) (*squares*), OHT (1 μM) (*circles*), or BBP (1 μM) (*triangles*), and the number of viable cells was counted. Data are shown as means ± S.D. of triplicate cultures.

conformation that enables the receptor to retain its ability to interact with corepressor to decrease the accessibility of AF-1 coactivators to the A/B region such that AF-1 activity is not efficiently activated.

Enhancement of the AF-1 Activity Stimulates Cancer Cell Growth—In a previous paper, we showed that the ERα(D351Y) mutant, which is derived from an MCF-7 breast tumor cell line that showed stimulated growth rather than inhibition by tamoxifen, exhibited reduced OHT-dependent interaction with corepressors to increase OHT-induced AF-1 activity compared with wild-type ERα (61). The AF-1 activity induced by BBP was comparable with that of OHT-bound ERα(D351Y), since BBP induced the binding of ERα to AF-1 coactivators but not to corepressors. These results raise the possibility that fully activated AF-1 induces the proliferation of breast cancer cells and that the binding of corepressors to ERα is essential for the antagonistic effect of OHT to inhibit proliferation of breast cancer cells. Therefore, we generated cell lines stably expressing ID1-2 region of N-CoR to abrogate OHT-dependent binding of ERα to corepressors. The stable transformants expressing the ID1-2 region exhibited the OHT-stimulated growth phenotype, indicating that the binding between OHT-occupied ERα and corepressors plays a key role in inhibition of tumor growth by tamoxifen. In addition, these results also indicate that fully activated AF-1 stimulates cancer growth.

Tamoxifen is an effective treatment for all stages of hormone-responsive breast cancer and can prevent breast cancer in high-risk women (44, 84). However, tamoxifen has a partial

estrogenic activity in the uterus and is associated with an increased incidence of endometrial hyperplasia and cancer. Recently, Brown and co-workers (75) showed that the expression level of SRC-1, a coactivator for ERα, is higher in an endometrial cancer cell line, Ishikawa, than in MCF-7. SRC-1 silencing by small interfering RNA in Ishikawa cells resulted in inhibition of tamoxifen-stimulated cell cycle progression. Hayashi and co-workers (85) reported that the relative transcriptional activity of AF-1 of ERα compared with that of AF-2 was 4-fold higher in Ishikawa cells than MCF-7 cells. They also mentioned that mitogen-activated protein kinase, which phosphorylates the serine residue at position 118 in ERα A/B domain, was constitutively activated in Ishikawa cells but not in MCF-7 cells. We reported previously (34–36) that the phosphorylation of serine 118 by mitogen-activated protein kinase stabilized the complex formation between ERα and p68/p72 DEAD box proteins, which are components of the p300/SRC-1 coactivator complex, to stimulate AF-1 activity of ERα. Together with these observations, our results suggest that the ratio between ERα AF-1-coactivator complex and ERα-corepressor complex in cells is an important determinant of AF-1 activity of OHT-occupied ERα and that the proliferation of cancer cells is regulated by AF-1 activity of OHT-bound ERα. From these observations, it is suggested that the tissue and cell type specificity of tamoxifen action is due to the difference of AF-1 activity of tamoxifen-bound ERα in various tissues and cells. Our results shed light on the molecular mechanism underlying tamoxifen-dependent inhibition of cancer growth and ring an alarm against endocrine disrupters.

Acknowledgments—We thank Dr. Akiyoshi Fukamizu and the members of his laboratory for providing materials and instruments for luciferase assay and Dr. Satoshi Nomoto for providing the MDA-MB-231 cell line.

REFERENCES

1. Evans, R. M. (1988) *Science* **240,** 889–895
2. Green, S., and Chambon, P. (1988) *Trends Genet.* **4,** 309–314
3. Tora, L., White, J., Brou, C., Tasset, D., Webster, N., Scheer, E., and Chambon, P. (1989) *Cell* **59,** 477–487
4. Lees, J. A., Fawell, S. E., and Parker, M. G. (1989) *Nucleic Acids Res.* **17,** 5477–5488
5. Ribeiro, R. C., Kushner, P. J., and Baxter, J. D. (1995) *Annu. Rev. Med.* **46,** 443–453
6. Katzenellenbogen, B. S. (1996) *Biol. Reprod.* **54,** 287–293
7. Parker, M. G. (1998) *Biochem. Soc. Symp.* **63,** 45–50
8. Danielian, P. S., White, R., Lees, J. A., and Parker, M. G. (1992) *EMBO J.* **11,** 1025–1033
9. Metzger, D., Ali, S., Bornert, J. M., and Chambon, P. (1995) *J. Biol. Chem.* **270,** 9535–9542
10. Lopez, G. N., Webb, P., Shinsako, J. H., Baxter, J. D., Greene, G. L., and Kushner, P. J. (1999) *Mol. Endocrinol.* **13,** 897–909
11. Kobayashi, Y., Kitamoto, T., Masuhiro, Y., Watanabe, M., Kase, T., Metzger, D., Yanagisawa, J., and Kato, S. (2000) *J. Biol. Chem.* **275,** 15645–15651
12. Beato, M., Herrlich, P., and Schutz, G. (1995) *Cell* **83,** 851–857
13. Horwitz, K. B., Jackson, T. A., Bain, D. L., Richer, J. K., Takimoto, G. S., and Tung, L. (1996) *Mol. Endocrinol.* **10,** 1167–1177
14. McKenna, N. J., Lanz, R. B., and O'Malley, B. W. (1999) *Endocr. Rev.* **20,** 321–344
15. Glass, C. K., and Rosenfeld, M. G. (2000) *Genes Dev.* **14,** 121–141
16. Chakravarti, D., LaMorte, V. J., Nelson, M. C., Nakajima, T., Schulman, I. G., Juguilon, H., Montminy, M., and Evans, R. M. (1996) *Nature* **383,** 99–103
17. Vo, N., and Goodman, R. H. (2001) *J. Biol. Chem.* **276,** 13505–13508
18. Yang, X. J., Ogryzko, V. V., Nishikawa, J., Howard, B. H., and Nakatani, Y. (1996) *Nature* **382,** 319–324
19. Onate, S. A., Tsai, S. Y., Tsai, M. J., and O'Malley, B. W. (1995) *Science* **270,** 1354–1357
20. Spencer, T. E., Jenster, G., Burcin, M. M., Allis, C. D., Zhou, J., Mizzen, C. A., McKenna, N. J., Onate, S. A., Tsai, S. Y., Tsai, M. J., and O'Malley, B. W. (1997) *Nature* **389,** 194–198
21. Hong, H., Kohli, K., Trivedi, A., Johnson, D. L., and Stallcup, M. R. (1996) *Proc. Natl. Acad. Sci. U. S. A.* **93,** 4948–4952
22. Anzick, S. L., Kononen, J., Walker, R. L., Azorsa, D. O., Tanner, M. M., Guan, X. Y., Sauter, G., Kallioniemi, O. P., Trent, J. M., and Meltzer, P. S. (1997) *Science* **277,** 965–968
23. Chen, H., Lin, R. J., Schiltz, R. L., Chakravarti, D., Nash, A., Nagy, L., Privalsky, M. L., Nakatani, Y., and Evans, R. M. (1997) *Cell* **90,** 569–580
24. Li, H., Gomes, P. J., and Chen, J. D. (1997) *Proc. Natl. Acad. Sci. U. S. A.* **94,** 8479–8484
25. Fondell, J. D., Ge, H., and Roeder, R. G. (1996) *Proc. Natl. Acad. Sci. U. S. A.* **93,** 8329–8333
26. Rachez, C., Suldan, Z., Ward, J., Chang, C. P., Burakov, D., Erdjument-Bromage, H., Tempst, P., and Freedman, L. P. (1998) *Genes Dev.* **12,** 1787–1800
27. Zamir, I., Harding, H. P., Atkins, G. B., Horlein, A., Glass, C. K., Rosenfeld, M. G., and Lazar, M. A. (1996) *Mol. Cell. Biol.* **16,** 5458–5465
28. Yuan, C. X., Ito, M., Fondell, J. D., Fu, Z. Y., and Roeder, R. G. (1998) *Proc. Natl. Acad. Sci. U. S. A.* **95,** 7939–7944
29. Rachez, C., Gamble, M., Chang, C. P., Atkins, G. B., Lazar, M. A., and Freedman, L. P. (2000) *Mol. Cell. Biol.* **20,** 2718–2726
30. McMahon, S. B., Van Buskirk, H. A., Dugan, K. A., Copeland, T. D., and Cole, M. D. (1998) *Cell* **94,** 363–374
31. Vassilev, A., Yamauchi, J., Kotani, T., Prives, C., Avantaggiati, M. L., Qin, J., and Nakatani, Y. (1998) *Mol. Cell* **2,** 869–875
32. Yanagisawa, J., Kitagawa, H., Yanagida, M., Wada, O., Ogawa, S., Nakagomi, M., Oishi, H., Yamamoto, Y., Nagasawa, H., McMahon, S. B., Cole, M. D., Tora, L., Takahashi, N., and Kato, S. (2002) *Mol. Cell* **9,** 553–562
33. Wang, L., Mizzen, C., Ying, C., Candau, R., Barlev, N., Brownell, J., Allis, C. D., and Berger, S. L. (1997) *Mol. Cell. Biol.* **17,** 519–527
34. Endoh, H., Maruyama, K., Masuhiro, Y., Kobayashi, Y., Goto, M., Tai, H., Yanagisawa, J., Metzger, D., Hashimoto, S., and Kato, S. (1999) *Mol. Cell. Biol.* **19,** 5363–5372
35. Watanabe, M., Yanagisawa, J., Kitagawa, H., Takeyama, K., Ogawa, S., Arao, Y., Suzawa, M., Kobayashi, Y., Yano, T., Yoshikawa, H., Masuhiro, Y., and Kato, S. (2001) *EMBO J.* **20,** 1341–1352
36. Kato, S., Endoh, H., Masuhiro, Y., Kitamoto, T., Uchiyama, S., Sasaki, H., Masushige, S., Gotoh, Y., Nishida, E., Kawashima, H., Metzger, D., and Chambon, P. (1995) *Science* **270,** 1491–1494
37. Pritchard, K. I. (2000) *Cancer (Phila.)* **88,** 3065–3072
38. Jobling, S., Reynolds, T., White, R., Parker, M. G., and Sumpter, J. P. (1995) *Environ. Health Perspect.* **103,** 582–587
39. Sonnenschein, C., and Soto, A. M. (1998) *J. Steroid. Biochem. Mol. Biol.* **65,** 143–150
40. Zacharewski, T. R., Meek, M. D., Clemons, J. H., Wu, Z. F., Fielden, M. R., and Matthews, J. B. (1998) *Toxicol. Sci.* **46,** 282–293
41. Picard, K., Lhuguenot, J. C., Lavier-Canivenc, M. C., and Chagnon, M. C. (2001) *Toxicol. Appl. Pharmacol.* **172,** 108–118
42. Fisher, B., Costantino, J. P., Wickerham, D. L., Redmond, C. K., Kavanah, M., Cronin, W. M., Vogel, V., Robidoux, A., Dimitrov, N., Atkins, J., Daly, M., Wieand, S., Tan-Chiu, E., Ford, L., and Wolmark, N. (1998) *J. Natl. Cancer Inst.* **90,** 1371–1388
43. Jordan, V. C. (1998) *Sci. Am.* **279,** 60–67
44. Levenson, A. S., and Jordan, V. C. (1999) *Eur. J. Cancer* **35,** 1628–1639
45. Lees, J. A., Fawell, S. E., and Parker, M. G. (1989) *J. Steroid Biochem.* **34,** 33–39
46. Berry, M., Metzger, D., and Chambon, P. (1990) *EMBO J.* **9,** 2811–2818
47. Gronemeyer, H., Benhamou, B., Berry, M., Bocquel, M. T., Gofflo, D., Garcia, T., Lerouge, T., Metzger, D., Meyer, M. E., Tora, L., Vergezac, A., and Chambon, P. (1992) *J. Steroid Biochem. Mol. Biol.* **41,** 217–221
48. McDonnell, D. P., Dana, S. L., Hoener, P. A., Lieberman, B. A., Imhof, M. O., and Stein, R. B. (1995) *Ann. N. Y. Acad. Sci.* **761,** 121–137
49. McInerney, E. M., Rose, D. W., Flynn, S. E., Westin, S., Mullen, T. M., Krones, A., Inostroza, J., Torchia, J., Nolte, R. T., Assa-Munt, N., Milburn, M. V., Glass, C. K., and Rosenfeld, M. G. (1998) *Genes Dev.* **12,** 3357–3368
50. van Leeuwen, F. E., Benraadt, J., Coebergh, J. W., Kiemeney, L. A., Gimbrere, C. H., Otter, R., Schouten, L. J., Damhuis, R. A., Bontenbal, M., Diepenhorst, F. W., van den Belt-Dusebout, A.W., and van Tinteren, H. (1994) *Lancet* **343,** 448–452
51. Morrow, M., and Jordan, V. C. (1993) *Arch. Surg.* **128,** 1187–1191
52. Wolf, D. M., and Jordan, V. C. (1993) *Breast Cancer Res. Treat.* **27,** 27–40
53. Tonetti, D. A., and Jordan, V. C. (1995) *Anti-Cancer Drugs* **6,** 498–507
54. Wolf, D. M., and Jordan, V. C. (1994) *Breast Cancer Res. Treat.* **31,** 129–138
55. Wolf, D. M., and Jordan, V. C. (1994) *Breast Cancer Res. Treat.* **31,** 117–127
56. Smith, C. L., Nawaz, Z., and O'Malley, B. W. (1997) *Mol. Endocrinol.* **11,** 657–666
57. Lavinsky, R. M., Jepsen, K., Heinzel, T., Torchia, J., Mullen, T. M., Schiff, R., Del-Rio, A. L., Ricote, M., Ngo, S., Gemsch, J., Hilsenbeck, S. G., Osborne, C. K., Glass, C. K., Rosenfeld, M. G., and Rose, D. W. (1998) *Proc. Natl. Acad. Sci. U. S. A.* **95,** 2920–2925
58. Zhang, X., Jeyakumar, M., Petukhov, S., and Bagchi, M. K. (1998) *Mol. Endocrinol.* **12,** 513–524
59. Shang, Y., Hu, X., DiRenzo, J., Lazar, M. A., and Brown, M. (2000) *Cell* **103,** 843–852
60. Jepsen, K., Hermanson, O., Onami, T. M., Gleiberman, A. S., Lunyak, V., McEvilly, R. J., Kurokawa, R., Kumar, V., Liu, F., Seto, E., Hedrick, S. M., Mandel, G., Glass, C. K., Rose, D. W., and Rosenfeld, M. G. (2000) *Cell* **102,** 753–763
61. Yamamoto, Y., Wada, O., Suzawa, M., Yogiashi, Y., Yano, T., Kato, S., and Yanagisawa, J. (2001) *J. Biol. Chem.* **276,** 42684–42691
62. Nagy, L., Kao, H. Y., Chakravarti, D., Lin, R. J., Hassig, C. A., Ayer, D. E., Schreiber, S. L., and Evans, R. M. (1997) *Cell* **89,** 373–380
63. Yanagisawa, J., Yanagi, Y., Masuhiro, Y., Suzawa, M., Watanabe, M., Kashiwagi, K., Toriyabe, T., Kawabata, M., Miyazono, K., and Kato, S. (1999) *Science* **283,** 1317–1321
64. Yanagi, Y., Suzawa, M., Kawabata, M., Miyazono, K., Yanagisawa, J., and Kato, S. (1999) *J. Biol. Chem.* **274,** 12971–12974
65. Zou, A., Marschke, K. B., Arnold, K. E., Berger, E. M., Fitzgerald, P., Mais, D. E., and Allegretto, E. A. (1999) *Mol. Endocrinol.* **13,** 418–430
66. Horlein, A. J., Naar, A. M., Heinzel, T., Torchia, J., Gloss, B., Kurokawa, R., Ryan, A., Kamei, Y., Soderstrom, M., Glass, C. K., and Rosenfeld, M. G. (1995) *Nature* **377,** 397–404
67. Seol, W., Mahon, M. J., Lee, Y. K., and Moore, D. D. (1996) *Mol. Endocrinol.* **10,** 1646–1655
68. Cohen, R. N., Wondisford, F. E., and Hollenberg, A. N. (1998) *Mol. Endocrinol.*

12, 1567–1581
69. Hu, X., and Lazar, M. A. (1999) *Nature* **402,** 93–96
70. Brzozowski, A. M., Pike, A. C., Dauter, Z., Hubbard, R. E., Bonn, T., Engstrom, O., Ohman, L., Greene, G. L., Gustafsson, J. A., and Carlquist, M. (1997) *Nature* **389,** 753–758
71. Shiau, A. K., Barstad, D., Loria, P. M., Cheng, L., Kushner, P. J., Agard, D. A., and Greene, G. L. (1998) *Cell* **95,** 927–937
72. Halachmi, S., Marden, E., Martin, G., MacKay, H., Abbondanza, C., and Brown, M. (1994) *Science* **264,** 1455–1458
73. Lemon, B. D., and Freedman, L. P. (1999) *Curr. Opin. Genet. & Dev.* **9,** 499–504
74. Chen, H., Tini, M., and Evans, R. M. (2001) *Curr. Opin. Cell Biol.* **13,** 218–224
75. Shang, Y., and Brown, M. (2002) *Science* **295,** 2465–2468
76. Wurtz, J. M., Bourguet, W., Renaud, J. P., Vivat, V., Chambon, P., Moras, D., and Gronemeyer, H. (1996) *Nat. Struct. Biol.* **3,** 87–94
77. Feng, W., Ribeiro, R. C., Wagner, R. L., Nguyen, H., Apriletti, J. W., Fletterick, R. J., Baxter, J. D., Kushner, P. J., and West, B. L. (1998) *Science* **280,** 1747–1749
78. Voegel, J. J., Heine, M. J., Zechel, C., Chambon, P., and Gronemeyer, H. (1996) *EMBO J.* **15,** 3667–3675
79. Heery, D. M., Kalkhoven, E., Hoare, S., and Parker, M. G. (1997) *Nature* **387,** 733–736
80. Ding, X. F., Anderson, C. M., Ma, H., Hong, H., Uht, R. M., Kushner, P. J., and Stallcup, M. R. (1998) *Mol. Endocrinol.* **12,** 302–313
81. Alland, L., Muhle, R., Hou, H., Jr., Potes, J., Chin, L., Schreiber-Agus, N., and DePinho, R. A. (1997) *Nature* **387,** 49–55
82. Li, J., Wang, J., Nawaz, Z., Liu, J. M., Qin, J., and Wong, J. (2000) *EMBO J.* **19,** 4342–4350
83. Huang, E. Y., Zhang, J., Miska, E. A., Guenther, M. G., Kouzarides, T., and Lazar, M. A. (2000) *Genes Dev.* **14,** 45–54
84. Jordan, V. C., Gapstur, S., and Morrow, M. (2001) *J. Natl. Cancer Inst.* **93,** 1449–1457
85. Sakamoto, T., Eguchi, H., Omoto, Y., Ayabe, T., Mori, H., and Hayashi, S. (2002) *Mol. Cell. Endocrinol.* **192,** 93–104
86. Castoria, G., Barone, M. V., Domenico, M. D., Bilancio, A., Ametrano, D., Migliaccio, A., and Auricchio, F. (1999) *EMBO J.* **18,** 2500–2510

Cell, Vol. 113, 905–917, June 27, 2003, Copyright ©2003 by Cell Press

The Chromatin-Remodeling Complex WINAC Targets a Nuclear Receptor to Promoters and Is Impaired in Williams Syndrome

Hirochika Kitagawa,[1,2] Ryoji Fujiki,[1] Kimihiro Yoshimura,[1] Yoshihiro Mezaki,[1] Yoshikatsu Uematsu,[1] Daisuke Matsui,[1] Satoko Ogawa,[1] Kiyoe Unno,[1,3] Mataichi Okubo,[3] Akifumi Tokita,[3] Takeya Nakagawa,[4] Takashi Ito,[4] Yukio Ishimi,[5] Hiromichi Nagasawa,[6] Toshio Matsumoto,[2] Junn Yanagisawa,[1,7] and Shigeaki Kato[1,7,*]

[1]Institute of Molecular and Cellular Biosciences
University of Tokyo
1-1-1 Yayoi
Bunkyo-ku
Tokyo 113-0032
Japan

[2]First Department of Internal Medicine
University of Tokushima School of Medicine
3-18-15 Kuramoto-cho
Tokushima 770-8503
Japan

[3]Department of Pediatrics
Juntendo University School of Medicine
3-1-3 Hongo
Bunkyo-ku
Tokyo 113-8431
Japan

[4]Department of Biochemistry
Nagasaki University School of Medicine
1-12-4 Sakamoto
Nagasaki 852-8523
Japan

[5]Mitsubishi Kagaku Institute of Life Sciences
11 Minamiooya
Machida-shi
Tokyo 194-8511
Japan

[6]Department of Applied Biological Chemistry
Graduate School of Agricultural and Life Sciences
University of Tokyo
1-1-1 Yayoi
Bunkyo-ku
Tokyo 113-0032
Japan

[7]SORST
Japan Science and Technology
4-1-8 Honcho
Kawaguchi
Saitama 332-0012
Japan

Summary

We identified a human multiprotein complex (WINAC) that directly interacts with the vitamin D receptor (VDR) through the Williams syndrome transcription factor (WSTF). WINAC has ATP-dependent chromatin-remodeling activity and contains both SWI/SNF components and DNA replication-related factors. The latter might explain a WINAC requirement for normal S phase progression. WINAC mediates the recruitment of unliganded VDR to VDR target sites in promoters, while subsequent binding of coregulators requires ligand binding. This recruitment order exemplifies that an interaction of a sequence-specific regulator with a chromatin-remodeling complex can organize nucleosomal arrays at specific local sites in order to make promoters accessible for coregulators. Furthermore, overexpression of WSTF could restore the impaired recruitment of VDR to vitamin D regulated promoters in fibroblasts from Williams syndrome patients. This suggests that WINAC dysfunction contributes to Williams syndrome, which could therefore be considered, at least in part, a chromatin-remodeling factor disease.

*Corresponding author: uskato@mail.ecc.u-tokyo.ac.jp

Introduction

Lipophilic ligands, such as fat-soluble vitamins A/D and thyroid/steroid hormones, exert their actions through transcriptional control of particular sets of target genes by direct binding and consequent activation of their cognate nuclear receptors (NRs) (Mangelsdorf et al., 1995). NRs form a superfamily and act as ligand-inducible regulators. From their functional and structural similarities, NR proteins are divided into five functional domains, designated A to E. The ligand binding domain (LBD) is located in the C-terminal E domain. The most conserved domain, C, is located in the NR center and serves as the DNA binding domain to specifically recognize and directly bind to their cognate ligand response elements in the target promoters. The LBD also harbors ligand-inducible transactivation function (AF-2). Upon ligand binding, NRs control transcription through ligand-dependent associations with a number of coregulators and coregulator complexes (Glass and Rosenfeld, 2000).

At transcriptional initiation sites in promoters, distinct classes of multiprotein complexes are thought to be indispensable for controlling transcription of sequence-specific regulators (Emerson, 2002; Narlikar et al., 2002). These complexes modify the chromatin configuration in a highly regulated manner, like nucleosome rearrangement, and bridge the functions between regulators and basal transcription factors, along with RNA polymerase II. Two major classes of chromatin-modifying complexes have been well characterized and their anchoring to the promoters presumably requires enzyme-catalyzed modifications of histone tails in chromatin (Hassan et al., 2002). One class contains several discrete subfamilies of transcription coregulatory complexes with either histone acetylase (HAT) or histone deacetylase (HDAC) activities to covalently modify histones through acetylation. In NR

ligand-induced transactivation processes, the complexes containing HDAC first act to corepress transactivation of unliganded NRs, while upon ligand binding, two HAT complexes, p160/CBP and TRRAP/GCN5, coactivate the NR function, like the other non-HAT DRIP/TRAP/SMCC coactivator complexes (Onate et al., 1995; Kamei et al., 1996; Rachez et al., 1998; Gu et al., 1999; Yanagisawa et al., 2002).

Another class of complexes uses ATP hydrolysis to rearrange nucleosomal arrays in a noncovalent manner and render chromosomal DNA accessible for sequence-specific regulators (Narlikar et al., 2002). These ATP-dependent chromatin-remodeling complexes act on transcription, DNA repair, and DNA replication and have been classified into subfamilies based on the major catalytic components with ATPase activity, SWI2/SNF2, ISWI, and Mi-2 (Fyodorov and Kadonaga, 2001; Yasui et al., 2002). These ATPases are highly conserved from yeast to humans and each forms a functionally similar, but distinct complex with a combination of specific components. However, the roles of most of the other components, except the catalytic subunits in chromatin remodeling, remain largely unknown (Narlikar et al., 2002).

Accumulating evidence revealed that both the chromatin-remodeling complexes and the coregulatory complexes cooperatively support transactivation of sequence-specific regulators like NRs (Glass and Rosenfeld, 2000; Emerson, 2002; Narlikar et al., 2002). However, the underlying molecular basis of the functional interplay among the complexes and the order of their recruitment through regulators to the promoters in controlling transcription at the specific local sites on the promoters are largely unknown.

Williams syndrome (WS) is a rare autosomal dominant hereditary disorder with multiple symptoms, including typically congenital vascular lesion, elfin face, mental retardation, and growth deficiency (Lu et al., 1998). Transient appearance of infantile aberrant vitamin D metabolism and hypercalcemia in the WS patients was also documented (Taylor et al., 1982; Garabedian et al., 1985). This syndrome is associated with genetic deletions at chromosome 7q 11.23, and several candidate genes in the deleted regions have been mapped from their mRNA expression levels (Hoogenraad et al., 2002). One gene, the Williams syndrome transcription factor (WSTF), has been suspected to be a candidate responsible for the diverse WS disorders (Lu et al., 1998; Peoples et al., 1998). This possibility is raised by the fact that WSTF is highly homologous to hACF1 as one of the WAC family proteins (Jones et al., 2000). Also, hACF1 is a partner of hSNF2h (a *Drosophila* ISWI homolog) to form well-characterized ISWI-based chromatin-remodeling complexes (Poot et al., 2000).

To search a chromatin-modifying complex to account for the ligand-independent occupancy of VDR in the target promoters, we purified from MCF7 cells a human multiprotein complex named "WINAC". The analysis of WINAC represents not only a molecular mechanism that a direct and selective interaction of a sequence-specific regulator with a chromatin-remodeling complex, but also the relationship between the function of WINAC and Williams syndrome disorders.

Results

Purification of a WSTF-Containing Multiprotein Complex Interacting with the VDR Ligand Binding Domain

To identify a coregulator complex for nuclear receptors, HeLa cell nuclear extracts were incubated with a chimeric VDR-DEF region protein (VDR-DEF) fused to glutathione-S-transferase (GST), in the presence or absence of 1α,25(OH)2D3 (Figure 1A). Proteins associated with VDR were collected under a milder washing condition (Yanagisawa et al. 2002) than that in the previous report (Rachez et al., 1998). Proteins that interacted with VDR-DEF were separated by SDS-PAGE and silver stained (Figure 1B). Mass spectrometry and the apparent molecular weights of the different proteins associated with the VDR-DEF in a ligand-dependent way led to the identification of several known components of the DRIP/TRAP/SMCC complex (Figure 1B), in agreement with previous observations (Rachez et al., 1998; Gu et al., 1999; Yanagisawa et al., 2002). One of the ligand-independent VDR-specific interactants was the Williams syndrome transcription factor (WSTF)/WBSCR9/BAZ1B (Lu et al., 1998; Peoples et al., 1998; Jones et al., 2000) (Figure 1B), and the WSTF protein was detected indeed in native HeLa cells (Figure 1C).

By Western blotting with specific antibodies, the NR coactivators, TRAP220 and TIF2, were detected only when VDR and ERα were liganded (Figure 1B). Unlike these factors, no ligand dependency, but VDR-selective interaction was found in WSTF (Figure 1B). By a GST pull-down assay, the physical and constitutive interaction of recombinant WSTF in vitro was observed for VDR-DEF irrespective of ligand binding, but not detected for ERα LBD (Figure 1D). In coimmunoprecipitations using the nuclear extracts of transfected MCF7 cells, WSTF appeared to interact with both unliganded and liganded VDR, while ligand-dependent recruitment of TRAP220 and TIF2 were expectedly seen for VDR as well as ERα (Yanagisawa et al., 2002) (Figure 1E).

To purify a WSTF-containing complex, we established a MCF7 stable transformant overexpressing FLAG-tagged WSTF. With the nuclear extracts of the stable transformants, WSTF containing complexes were isolated by multistep purification using the GST-VDR column and an anti-FLAG affinity resin column (Figure 2A). On the glycerol density gradient (Figure 2B, upper image), the purified complexes with a molecular weight of greater than 670 kDa bound to the GST-VDR column and these large molecular weight fractions contained WSTF, indicating that WSTF forms a stable nuclear complex. The fractions containing FLAG-tagged WSTF were then applied on the anti-FLAG affinity column to isolate the complex.

Identification of a WSTF Complex

With the mass fingerprinting, we identified all the components of the purified complex containing WSTF (Figure 2C), and designated this complex as WINAC (*W*STF *I*ncluding *N*ucleosome *A*ssembly Complex). WINAC stable formation was further supported by coimmunoprecipitation with a CAF-1p150 antibody (Figure 2C). WINAC consists of at least 13 components, but unexpectedly

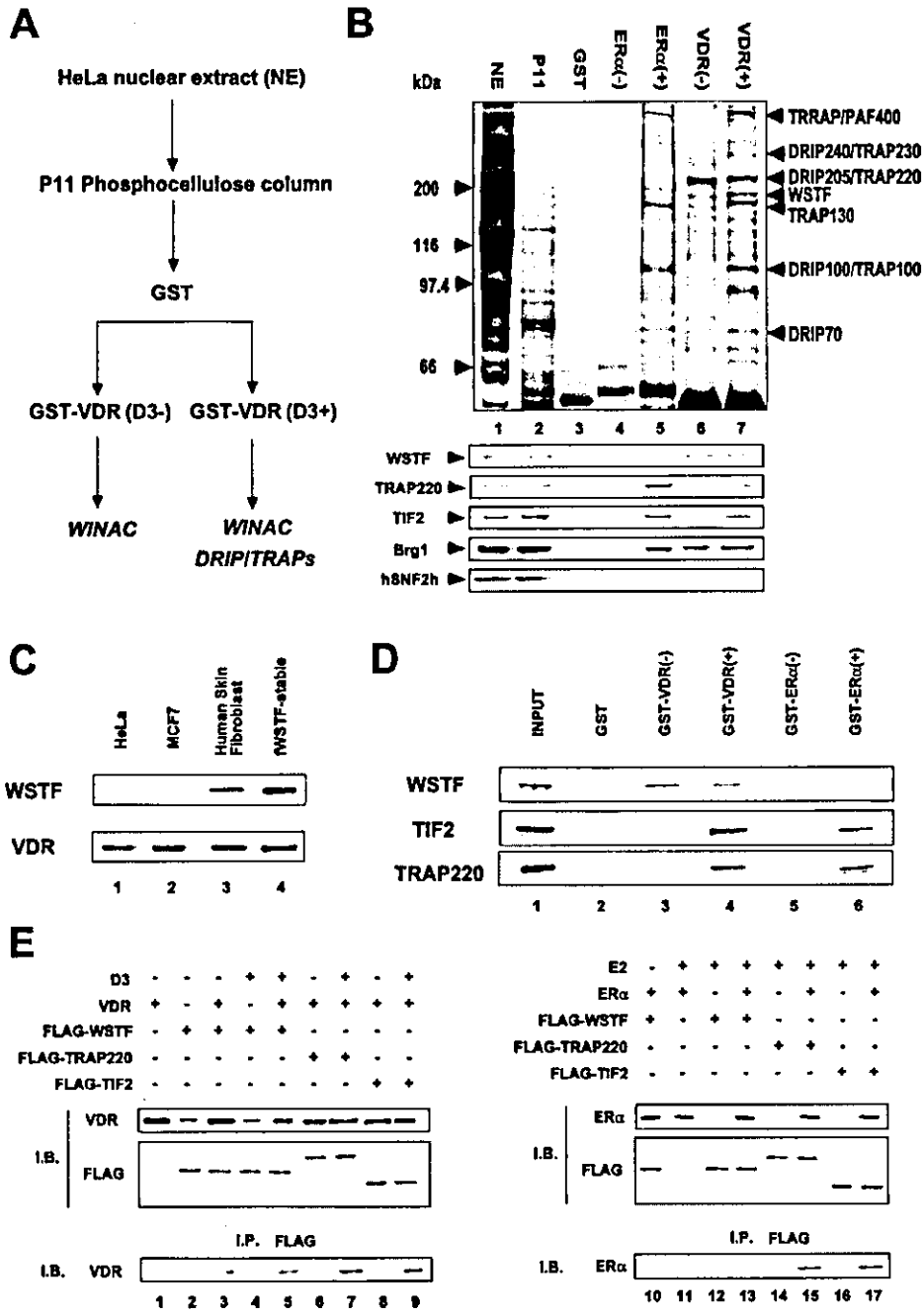

Figure 1. Purification and Identification of Human Proteins Interacting with 1α,25(OH)2D3, Unbound and Bound VDR

(A) Purification scheme for VDR interacting proteins. The eluted fraction from P11 phosphocellulose column was incubated with immobilized GST-VDR(DEF) in the absence or presence of 1α,25(OH)2D3(D3,10^{-6} M).

(B) Identification of ligand-independent and -dependent VDR interacting proteins. In the upper image, fractions were subjected to SDS-PAGE, followed by silver staining. Total HeLa S3 nuclear extract [NE] (lane 1), a fraction eluted from the P11 column [p11] (lane 2), fractions from GST [GST] (lane 3), unliganded- and liganded-GST-ERα(DEF) columns [ERα(−);ERα(+)] (lanes 4 and 5), unliganded- and liganded-GST-VDR(DEF) columns [VDR(−);VDR(+)] were examined by mass spectrometry and identified proteins are indicated at the right side of the image. The lower image shows Western blot analysis using specific antibodies shown in the image.

(C) Protein expression in cultured cells. Western blotting with antibodies against WSTF or VDR was performed with indicated cell lines (3 × 10^5 cells/lane).

(D) Direct and ligand-independent interaction of WSTF with VDR in vitro. WSTF, TIF2, and TRAP220 were translated in vitro and incubated with a receptor-GST chimeric protein immobilized on glutathione-Sepharose beads in the presence or absence of the cognate ligands.

(E) 1α,25(OH)2D3-independent interaction between VDR and WSTF in vivo. The upper image displays the Western blot of the total cell extracts (Yanagisawa et al., 2002) to verify expression. The lower image shows the Western blot of the immunoprecipitates by anti-FLAG M2-affinity resin to detect the receptor.

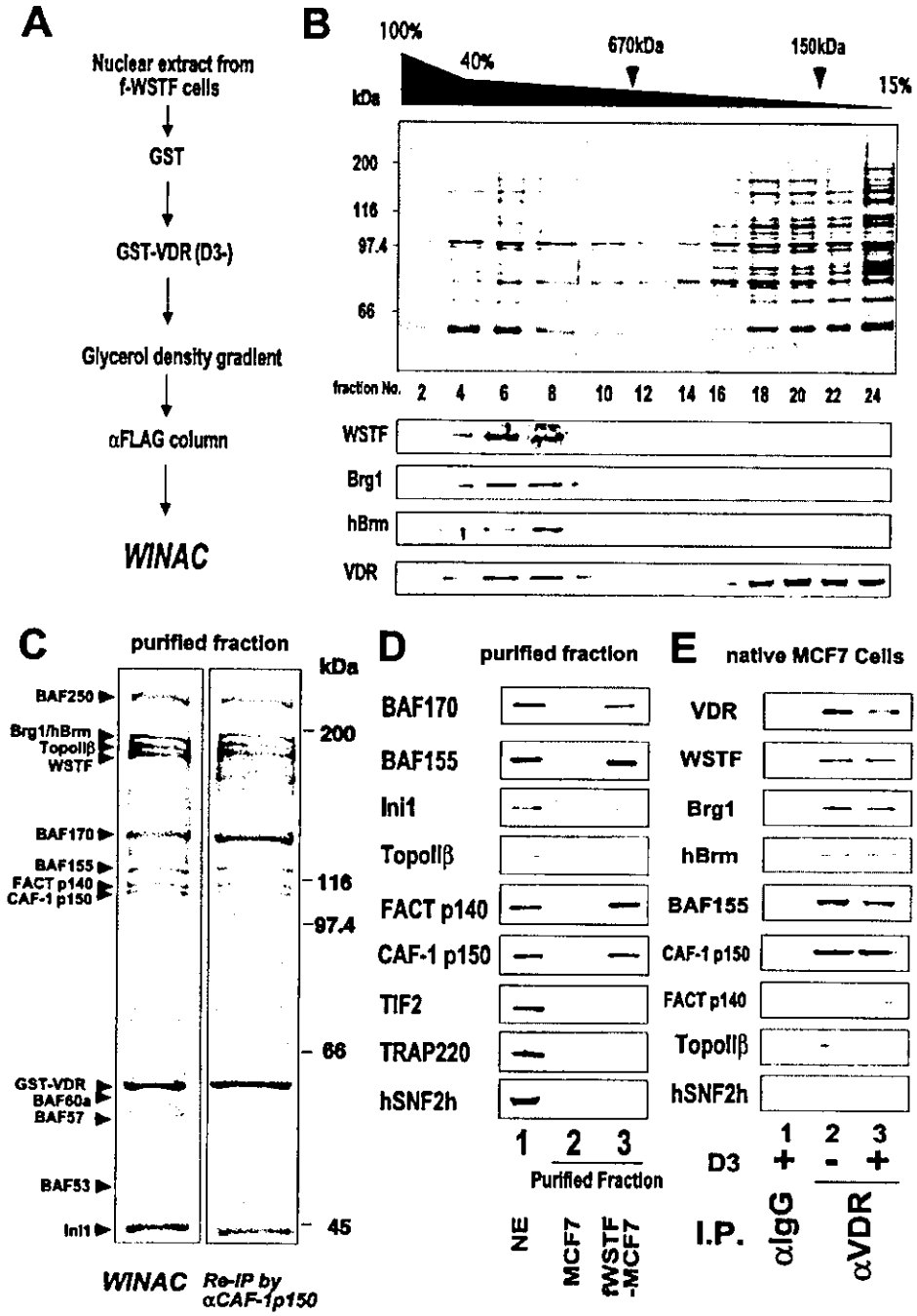

Figure 2. Purification and Identification of a Human WSTF-Containing Multiprotein Complex "WINAC"

(A) Purification scheme of WINAC from MCF7 stable transformants (Yanagisawa et al., 2002).

(B) Fractionation of purified complexes on glycerol density gradient. In the lower image, Western blot analysis of each fraction using specific antibodies is shown.

(C) The purified complex was subjected to SDS-PAGE, followed by silver staining and identified by mass spectrometry (left image). The right image shows the reimmunoprecipitation (Re-IP) of purified WINAC by the anti-CAF-1 p150 antibody.

(D) Western blot analysis of WINAC. Western blot analysis was performed to compare nuclear extracts (lane 1), mock MCF7 (lane 2), and FLAG-WSTF stable transformants containing WINAC (lane 3) with specific antibodies.

(E) Detection of endogenous WINAC components by Western blotting.

contains neither hSNF2h nor the components of known ISWI-based complexes (Figure 2C). Rather, the SWI/SNF type ATPases (Brg1 and hBrm) and several BAF components share with the SWI2/SNF2-based complexes (Narlikar et al., 2002). However, we could not detect BAF180, which is specific to one of the hSWI/

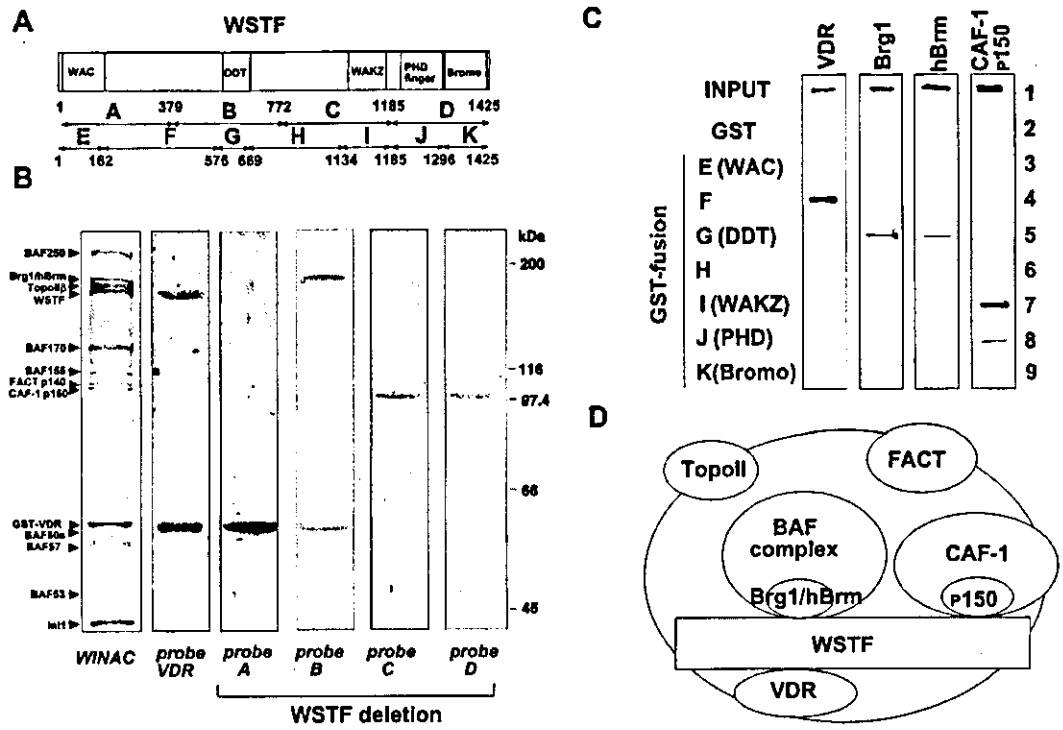

Figure 3. WSTF as a Platform Protein in WINAC

(A) Schematic representation of the probes used for the Far Western blotting and the GST pull-down assay. WSTF deletion mutants are expressed as GST-chimeric proteins.

(B) Far Western blotting of the WINAC complex probed with indicated ^{32}P-labeled GST-fused chimeric proteins. ^{32}P-labeled GST-fused chimeric proteins were prepared with pGEX-2TK vector (Amersham Biosciences) by PKA phosphorylation (Rachez et al., 1998).

(C) Physical interaction of WINAC components and VDR with WSTF deletion mutants in GST pull-down assay.

(D) Schematic representation of the interacting domains of WSTF.

SNF-type complexes, PBAF, which was purified and identified by in vitro transcription to coactivate VDR in a ligand-dependent manner (Lemon et al., 2001). Interestingly, WINAC appears to harbor three components (TopoIIβ, FACTp140, and CAF-1p150) (Smith and Stillman, 1989; Varga-Weisz et al., 1997; LeRoy et al., 1998), which have not yet been found in any known ATP-dependent chromatin-remodeling complexes. Western blotting with specific antibodies verified several WINAC components (Figure 2D). Moreover, major WINAC components in a purified endogenous complex associating with VDR were detected (Figure 2E), supporting presence of WINAC as a stable complex in native cells.

Clear retention of VDR was detected upon the WSTF band, but not the other subunits (Figure 3B), confirming the GST-pull-down assay results (Figure 1D). The WSTF fragments were trapped on not only VDR but also CAF-1p150 and Brg1/hBrm (Figure 3B). Such interactions were also seen in the expected regions by the GST-pull-down assay (Figure 3C), suggesting that WSTF serves as a platform subunit to assemble components into WINAC (as illustrated in Figure 3D).

WINAC Is a Multifunctional ATP-Dependent Chromatin-Remodeling Complex

We then examined if purified WINAC exerts an ATP-dependent chromatin-remodeling activity by comparing its activity with a complex of the recombinant dAcf1 and dISWI proteins in a standard micrococcal nuclease assay. This recombinant complex has been reported sufficient to mobilize nucleosomes in vitro in an ATP-dependent manner (Ito et al., 1997). Like the dISWI complex, an ATP-dependent chromatin-assembly reaction was clearly induced by WINAC (compare lanes 6, 7, and lane 3 in Figure 4A), indicating that Brg1/hBrm in WINAC serves as an ATPase for this ATP-dependent chromatin-remodeling process. WINAC appeared to have a chromatin-assembly activity (data not shown) like RSF (Loyola et al., 2001).

We then examined the ability of WINAC to disrupt nucleosome arrays through VDR bound DNA since the known ATP-dependent chromatin-remodeling complexes are potent to recognize the nucleosomal array around the binding sites of a sequence-specific regulator (Ito et al., 1997; Lemon et al., 2001). By Southern blot analysis with a pair of oligonucleotides complementary to a region in the vicinity (promoter probe) or to a site about 900 bp upstream (distal probe) of the GAL4 DBD binding sites for a chimeric VDR-DEF protein (GAL-VDR), disruption of the nucleosome arrays in the GAL4 binding site vicinity was induced only when both VDR and WINAC were present (lane 4 in Figure 4B), while the other regions appeared unaffected in the nucleosome arrays (Figure 4B). Reflecting the VDR-specific nucleo-

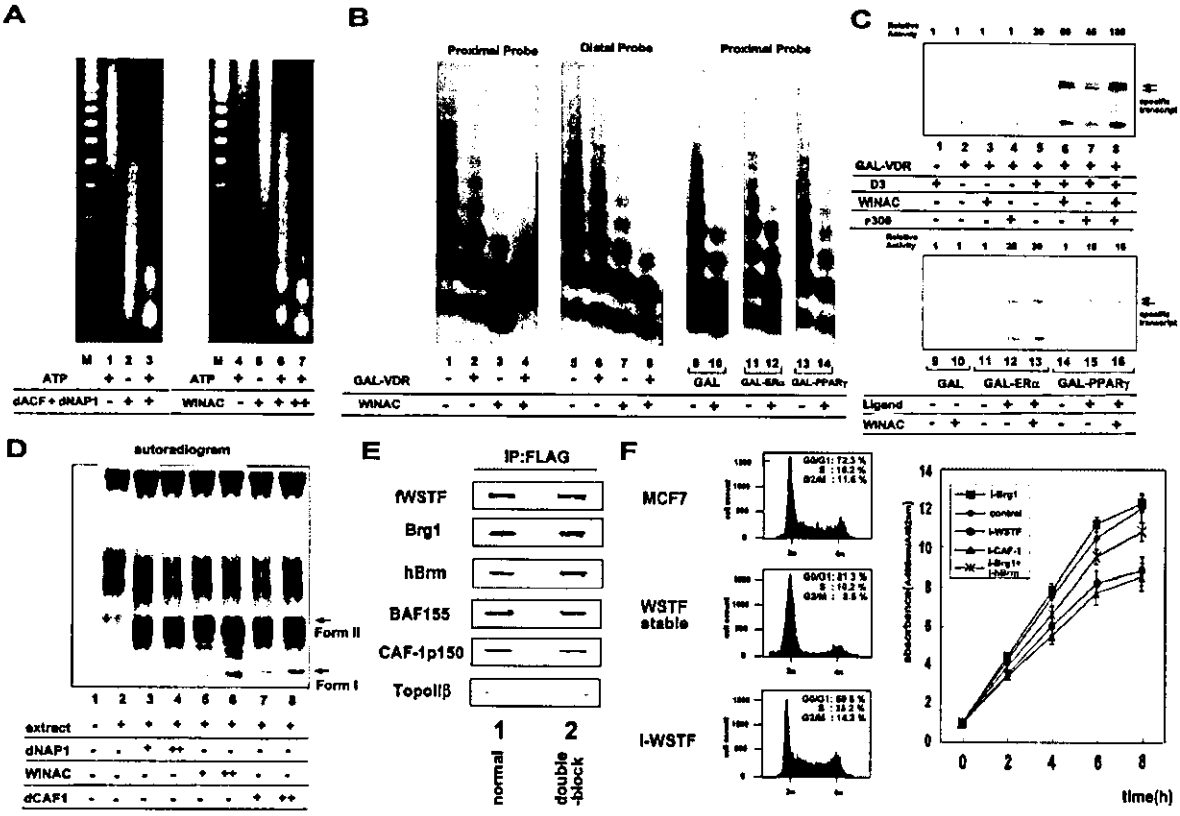

Figure 4. WINAC as an ATP-Dependent Chromatin-Remodeling Complex

(A) Chromatin-reconstitution activity of WINAC. The reacted samples were subjected to partial micrococcal nuclease digestion. The molecular mass marker (M) is the 200 bp ladder.

(B) Chromatin disruption by WINAC is specifically VDR dependent. Oligonucleotide probe corresponds to either a sequence between the GAL4 sites and the RNA start site (proximal probe) or 900 bp upstream of the start site (distal probe).

(C) Potentiation of VDR transactivation by WINAC in vitro. Arrows indicate specific transcripts by transcription reactions by GAL4 derivatives. A representative result is displayed, and relative activities were calculated from three independent assays with pGl0 vector as an internal control.

(D) WINAC functions as a chromatin-reconstitution factor during DNA replication in vitro. During DNA replication induced by SV40 T antigen in vitro, WINAC could form chromatin with negatively supercoiled DNA. Form I, a perfect supercoiled DNA; form II, a relaxed form.

(E) WINAC formation is unchanged in S phase. MCF7 stable transformants were cultured under either normal conditions or double-thymidine block treatments.

(F) Modulation of the cell cycle by altered WSTF expression. Left image: DNA histogram of the MCF7 cells [MCF7], WSTF stably expressing MCF7 cells [WSTF stable] and MCF7 cells transfected with WSTF-RNAi [i-WSTF]. Right image: BrdU incorporation during S phase of the MCF7 cells transfected with RNAi from the indicated proteins during double-thymidine treatment. After the final release (time 0), cells were collected every 2 hr, for up to 8 hr. The average values of triplicate analyses are shown.

some disruption by WINAC among tested receptors (Figure 4B), ligand-induced transactivation in vitro was potentiated by WINAC for VDR, but for neither ERα nor PPARγ (Figure 4C).

WINAC Function during DNA Replication

The WINAC function in DNA replication (Smith and Stillman, 1989; Varga-Weisz et al., 1997) was addressed by reconstituting chromatin structure upon newly replicated DNA by an in vitro assay. WINAC, like the reported CAF-1 histone chaperone complex (see lanes 7 and 8 in Figure 4D), could facilitate forming chromatin structure with negatively supercoiled DNA on newly replicated DNA through nucleosome arrangement (Smith and Stillman, 1989) (Figure 4D). Moreover, WINAC complex formation was detected irrespective of the cell-cycle stages, even when blocked at S stage by double-thymidine treatments (Fujita et al., 1996) (Figure 4E). Manipulation of WSTF expression by WSTF-RNAi expression (Elbashir et al., 2001) resulted in alterations in the cell cycle (left images in Figure 4F). Particularly, DNA synthesis was clearly lowered by RNAi expression of either WSTF or Brg1/hBrm ATPases (right image in Figure 4F). Thus, these findings suggest that WINAC plays a role in chromatin remodeling during DNA replication.

WSTF Coactivated Ligand-Induced Transactivation Function of VDR

Next, we investigated if WSTF potentiates the ligand-induced transactivation of VDR in MCF7 cells by transient expression analysis. 1α,25(OH)2D3 (10^{-9} M) was effective to induce VDR AF-2 transactivation function.

WSTF coactivated this ligand-induced AF-2 function of VDR, but not ERα (compare lanes 3 and 4 with 23 and 24 in Figure 5A). Both Brg1 and hBrm were potent to enhance the transactivation functions of VDR and ERα (compare lanes 9 and 12 with lane 2 for VDR; lanes 29 and 32 with lane 22 for ERα in Figure 5A) as previously reported (Chiba et al., 1994; DiRenzo et al., 2000; Shang et al., 2000; Belandia et al., 2002). Interestingly, such coactivator-like activity of WSTF was selective for VDR, and not detected for ERα, even in the presence of Brg1/hBrm (see lanes 30 and 33 in Figure 5A).

To confirm such a coactivator-like function of WSTF for VDR, the ligand-induced transactivation function of VDR was assessed 40 hr after the RNAi transfection and was severely attenuated nearly to basal transcription levels (lanes 7 and 8 in Figure 5A). Interestingly, WSTF-RNAi expression was found to also abrogate the VDR coactivation of the VDR transcriptional activity by the known NR coactivators, such as TRAP220 and TIF2 (lanes 16 and 18 in Figure 5A). Similarly, RNAi expression resulted in a loss of the coactivator-like function of WSTF for VDR when intact VDR/RXR heterodimer was bound to a naturally occurring positive vitamin D response element (VDRE) derived from the human 1α,25-dihydroxyvitamin D3 24-hydroxylase [24(OH)ase] gene promoter (Chen and DeLuca, 1995) (Figure 5C). ChIP analysis revealed that VDR and the WINAC components were constitutively associated with the promoter irrespective of ligand binding. In the contrast, ligand-induced occupancy in the promoter was seen in TRAP220 and TIF2 with ligand-induced histone H4 acetylation (compare lane 3 with 4 in Figure 5B), though the ligand-induced TRAP220 and TIF2 occupancy was cyclic (data not shown) as expected from previous reports (Shang et al., 2000). Such ligand-dependent and -independent recruitments of factors to the promoter were robustly attenuated by WSTF-RNAi expression (lane 5 in Figure 5B).

As the VDR/RXR heterodimer also represses transcription in a ligand-dependent manner through negative VDRE (nVDRE), the action of WSTF in the ligand-induced transrepression was examined in a naturally occurring nVDRE in human 25-hydroxyvitamin D3 1α-hydroxylase [1α(OH)ase] (Murayama et al., 1998). ChIP analysis uncovered that VDR and WINAC appear to land on the nVDRE in a ligand-independent manner, while ligand-induced (compare lane 8 with 9 in Figure 5B), but cyclic (data not shown) recruitments of N-CoR and HDAC2 were observed. Ligand-dependent repression was exaggerated by WSTF overexpression (lanes 3 and 4 in Figure 5D), but attenuated again by WSTF-RNAi expression (lanes 5 and 6 in Figure 5D). Thus, it is likely that WINAC association with VDR facilitates targeting of a putative corepressor complex to the nVDRE. The WINAC function in the native VDR target gene promoters and the endogenous gene expressions of 24(OH)ase and 1α(OH)ase were further confirmed by the impaired 1α,25(OH)2D3 responsiveness by the WSTF ablation (Figure 5E). Thus, these findings point out that WINAC rearranges the nucleosome array around the positive and negative VDREs, thereby facilitating the coregulatory complexes accessible to VDR for further transcription control.

Impaired Transactivation Function of VDR Was Recovered by WSTF Overexpression in Williams Syndrome Patients

Together with these observations, the typical phenotypes of the WSTF gene-deleted WS patients (Taylor et al., 1982; Garabedian et al., 1985) prompted us to assume that a lowered WINAC function caused by reduced WSTF expression may result in aberrant chromatin remodeling, leading to diverse abnormalities, including abnormal vitamin D metabolism and hypercalcemia. Considering WSTF and VDR skin expression (Yoshizawa et al., 1997), we first assessed the ligand-induced transactivation function of VDR in skin fibroblast cells derived from three normal and three WS patients, in which the region covering the WSTF gene is deleted in one chromosome 7 allele, as representatively shown in patient #1 by FISH analysis (Figure 6A). Northern blot analysis unmasked the WSTF expression levels were clearly lowered (~50%) in the WS patients (Figure 6B). By a transient transfection assay in fibroblast cells, we found reduced transactivation function of VDR in the WS patient cells (Figure 6C). Consistent with the impaired function of VDR in the WS cells, the ChIP analysis showed robust reduction in targeting of VDR, the WINAC components, and the coactivators to the 24(OH)ase VDRE (lanes 9 and 10 in Figure 6E), in agreement with the MCF7 cell results (Figure 5B).

Most strikingly, WSTF expression by an adenovirus vector (Kitagawa et al., 2002) could rescue the reduced responsiveness of 24(OH)ase gene induction by 1α,25(OH)2D3 for 12 hr in the WS skin fibroblasts (compare lane 3 with 4 in Figure 6D), with the impaired promoter targeting of the WINAC components and unliganded recoveries in VDR to the 24(OH)ase promoter (see lane 11 in Figure 6E), and the impaired ligand-induced recruitment of the NR coactivators (see lane 12 in Figure 6). Thus, these findings suggest that at least a part of the endocrine disorders found in the WS patients are related to VDR malfunction caused by the lowered WINAC function, which is due to lower WSTF expression.

The WSTF transcript during embryogenesis was not detected by Northern blotting, but detectable by RT-PCR (Figure 7A). By whole mount in situ staining (Sekine et al., 1999) at 9.5 dpc, the WSTF transcript appeared to be ubiquitously expressed (data not shown), but its expression pattern became limited and partially overlapped with mouse Brg1 and BAF155 (Srg3) expression (Bultman et al., 2000; Kim et al., 2001) as evident at 11.5 dpc (Figure 7B). Surprisingly these expression patterns seem different from that of mouse Snf2h (Lazzaro and Picketts, 2001), particularly at brain. These results may suggest a specific role of WINAC during embryogenesis, which may account for the diverse abnormalities in the WS patients.

Discussion

Purification and Identification of a Human Multiprotein Complex Containing WSTF, WINAC

WINAC contains known components of the hSWI/SNF-type complexes, including two major ATPase subunits, Brg1 and hBrm (Figure 2C). However, by our purification

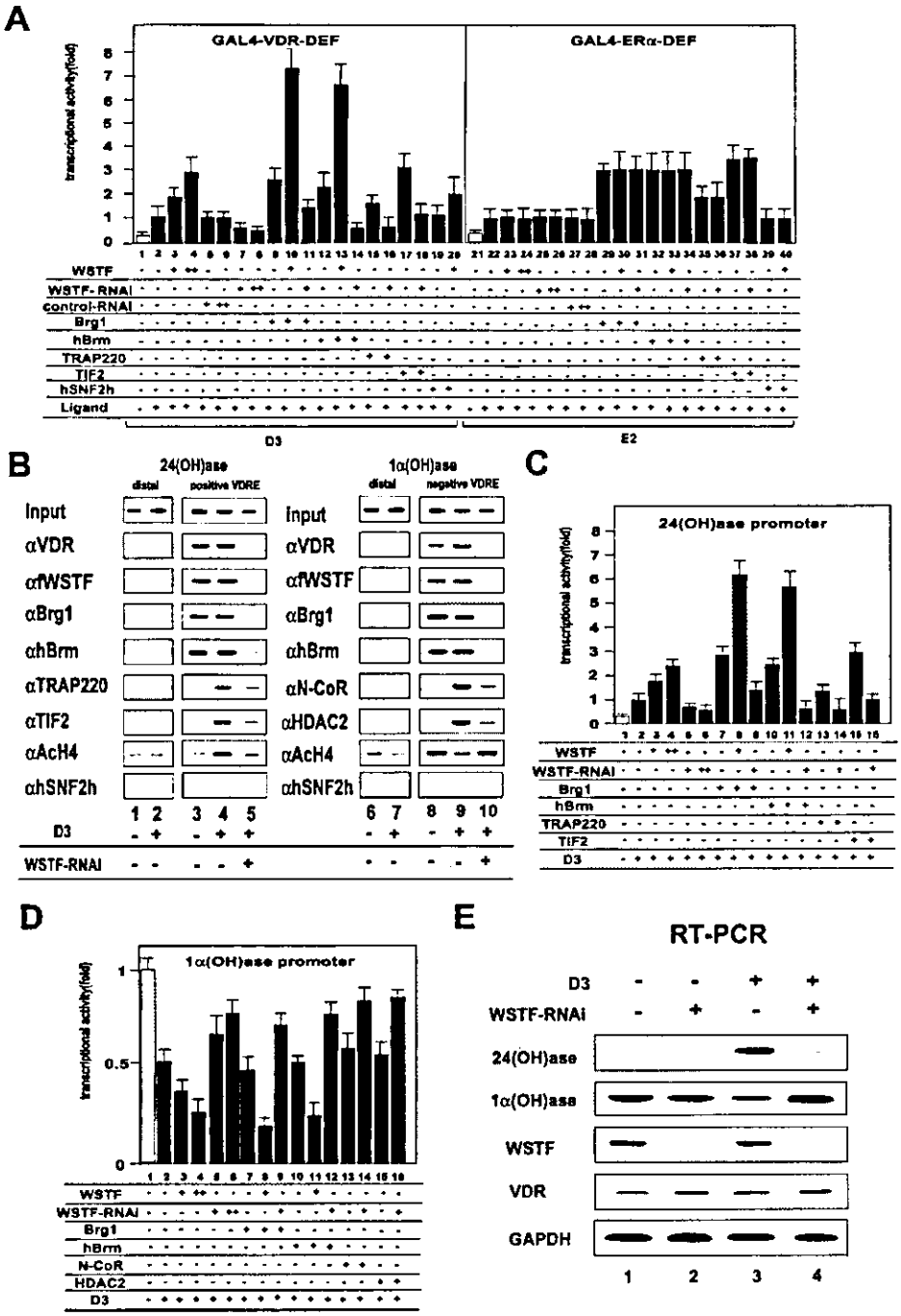

Figure 5. Ligand-Dependent Promoter Targeting of Coregulators through WINAC-VDR Association

(A) VDR-specific facilitation of co-activator accessibility by WINAC. MCF7 cells were transfected with the expression vectors of a luciferase reporter plasmid containing the GAL4 upstream activation sequence (UAS) [17mer(×2)] driven by the β-globin promoter (0.5 μg). PML-CMV (2 ng); GAL4-DBD-VDR-DEF (0.2 μg); GAL4-DBD-ERα DEF (0.2 μg); pDNA3-FLAG-WSTF (+; 0.1 μg: ++; 0.3 μg); pSV-Brg1 (0.2 μg); pSV-hBrm (0.2 μg); pcDNA3-TRAP220 (0.3 μg); pcDNA3-TIF2 (0.3 μg); siRNA (+; 0.1 μg: ++; 0.2 μg) of WSTF-RNAi; or control RNAi or their combinations were transfected as indicated in the images in the absence or presence of ligand (10^{-9} M). Bars in each graph show the fold change in luciferase activity relative to the activity of the receptor transactivation in the presence of ligand.

(B) ChIP analysis on the 24(OH)ase promoter and 1α(OH)ase promoter of WSTF stable transformants. Soluble chromatin was prepared from WSTF stable transformants treated with D3 (10^{-9} M) for 45 min and immunoprecipitated with indicated antibodies.

(C and D) The coregulator-like actions of WSTF on the naturally occurring positive and negative vitamin D response elements. MCF7 cells were transfected with the expression vectors of either the luciferase reporter plasmid containing a human 24(OH)ase promoter harboring a canonical positive VDRE or a human 1α(OH)ase promoter containing a negative VDRE and the factors shown in (A) or together with pcDNA3-N-CoR (0.3 μg), pcDNA3-HDAC2 (0.3 μg).

(E) WSTF-mediated regulations of endogenous genes by VDR. RT-PCR analysis of MCF7 cells was performed 12 hr after the induction by D3 (10^{-9} M) (Yanagisawa et al., 2002).

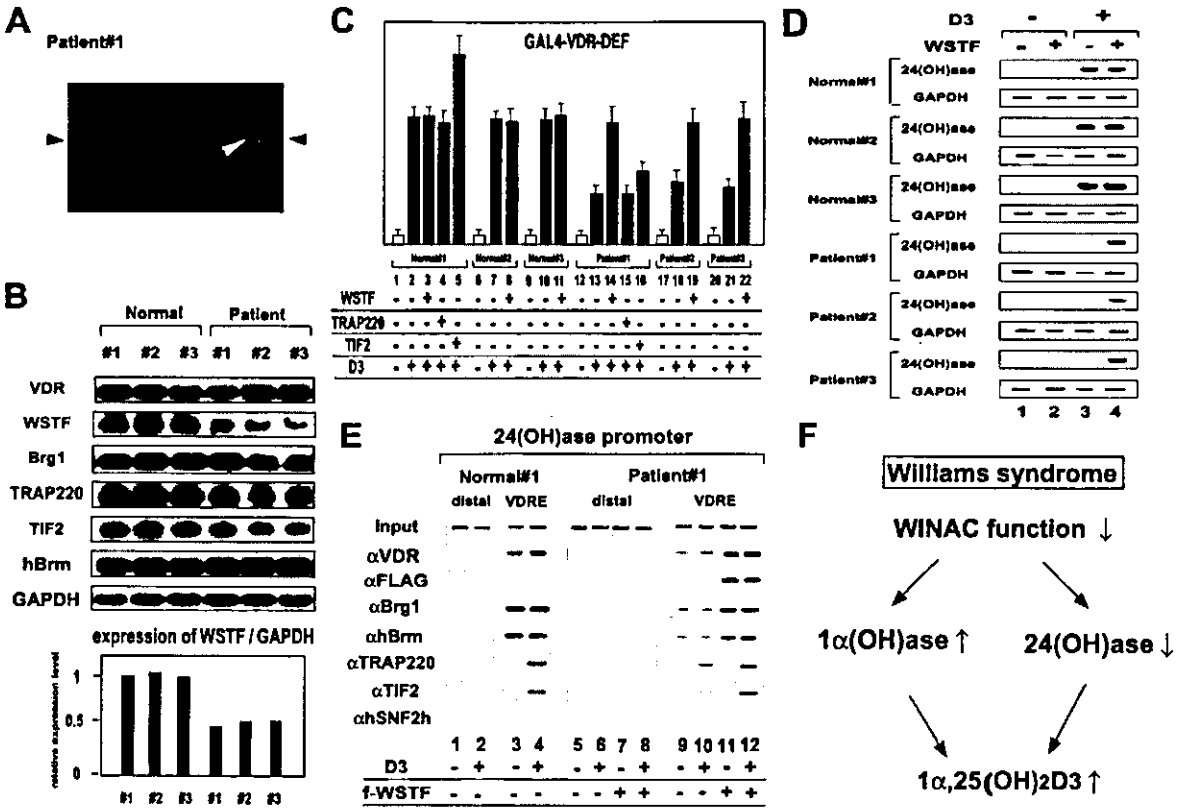

Figure 6. Impaired VDR Function in the Fibroblasts of Williams Syndrome Patients Was Recovered by WSTF Overexpression

(A) Fluorescence in situ hybridization of WS patient 1, confirming a deletion of one copy of the WSTF gene. The black arrowhead indicates D7S427 gene locus and the white arrowhead for WSTF gene. D7S427 was used for a chromosome 7 marker and cosmid full-length WSTF for WSTF gene probe.

(B) Reduced WSTF expression levels in WS skin fibroblasts. The indicated genes were examined for expression by Northern blotting with GAPDH expression as an internal control (Yanagisawa et al., 2002). Densitometric analysis of the relative expression level of WSTF versus GAPDH is shown in the lower image.

(C) VDR transactivation functions were impaired in the skin fibroblasts of the WS patients. Fibroblasts from controls and patients were transfected with the expression vectors as described in Figure 5A and the receptor function was tested.

(D) WSTF overexpression recovered the impaired responsiveness to vitamin D during 24(OH)ase gene induction. Patient's skin fibroblasts were transfected with an adenovirus expressing FLAG-WSTF, and treated with 1α,25(OH)2D3 (10^{-9} M) for 12 hr. Total RNA was subjected to RT-PCR analysis of 24(OH)ase expression.

(E) Impaired promoter targeting of VDR, coregulators, and WINAC components in fibroblasts from WS patients was rescued by WSTF overexpression. ChIP assays of the patient skin fibroblasts were performed with adenovirus expressing FLAG-WSTF as described in Figure 5B.

(F) Hypothesis of the cause of hypercalcemia in Williams syndrome patients.

methods we could detect neither the PBAF complex nor its specific component (BAF180). Moreover, by our purification, no ISWI-based complex was detectable even in the glycerol gradient fractions containing complexes with expected molecular weights. These observations are also different from a report that WSTF forms a hISWI-based chromatin-remodeling complex (Bozhenok et al., 2002). Confirming that hISWI (hSNF2h) expression did not affect the VDR transactivation function (Figures 5A and 5B), the combination with ISWI-based complex components looks to deter WSTF from the VDR interaction.

Of note, WINAC harbors three components, which have not yet been found in the ATP-dependent chromatin-remodeling complexes. Two factors (CAF-1p150 and TopoIIβ are integrated in the complexes serving roles in DNA replication (Smith and Stillman, 1989; Varga-Weisz et al., 1997), while FACT p140 is involved in a complex that promotes chromatin-dependent transcriptional elongation with an ISWI-type complex (LeRoy et al., 1998). From the observed WSTF interactions with the other subunits in vitro (Figures 3A–3D), WSTF appears to serve as a core protein to form an SWI2/SNF2-based complex, generating a subclass of the ATP-dependent chromatin-remodeling complex with DNA replication-related factors. Taken together, WSTF may serve as a dual platform protein capable of forming both SWI/SNF- and ISWI-type chromatin-remodeling complexes by distinct subunit combinations, but only the SWI/SNF-type WINAC selectively assists VDR function through a physical interaction.

WINAC Is a Chromatin-Remodeling Complex

Specific and more efficient targeting of VDR through WINAC to the VDREs was supported from functional analyses of the purified WINAC in vitro. In this respect,